

Authors' response to anonymous referee #1 on "Enhanced Stratospheric Water Vapor over the Summertime Continental United States and the Role of Overshooting Convection" by R. L. Herman et al., ACP-2016-1065

We would like to thank the referee #1 for detailed review, and for insightful and constructive comments. This response replaces the previous authors' comment (in January 2017). This response addresses all of the referee's individual points below:

#### Major Comment

##### Referee's Major Comment:

"In my opinion this paper could easily stand alone if all Figures and in-depth discussions of Aura MLS stratospheric water vapor measurements were omitted. The vast majority of scientific conclusions can be made without the broader picture provided by the MLS data. The one significant contribution of MLS data to this paper is to show the low frequency of occurrence of anomalously high stratospheric water vapor mixing ratios over the North American monsoon region. However, this conclusion, based on MLS water vapor data, was already published by Schwartz et al. (2013, Geophys. Res. Lett.). There are also some difficulties translating between the aircraft and MLS results because of the presumably different mixing ratio thresholds used to identify "enhanced" water vapor for each. Intuitively the MLS threshold needs to be lower because of the much coarser vertical and horizontal resolution of MLS retrievals. See my comments below regarding this issue."

"I will leave it up to the authors if they want to retain or omit the MLS data in their paper. I don't think its presence detracts from the main objectives of this paper, but I also think it doesn't contribute much to them."

##### Authors' Response to Major Comment:

The Aura MLS stratospheric water vapor measurements place the aircraft field mission data into regional and decadal perspective. We have improved the text and figures (as described below) to tie MLS and the aircraft results together. MLS helps us address the question from Toon et al (2016): "Do deep convective cloud systems locally inject water vapor and other chemicals into the overworld stratosphere over the CONUS?"

We do agree with the referee that our old Figure 1 (MLS 2004-2013 time series) is similar to a previously published figure (MLS 2004-2012 time series from Schwartz et al., 2013), and will be removed from the revised paper.

##### Authors' Changes in Manuscript in response to Major Comment:

The old Figure 1 (MLS decadal time series) has been replaced by a histogram of MLS water (new Figure 4). Also, in our revised paper we show that both MLS water at 100 hPa and aircraft water are enhanced significantly above background with revised plots of both aircraft and MLS data (Figures 1, 4 and 6).

## Minor Comments

### Referee's Minor Comment 1)

Figure 1 and Caption. "Each monthly histogram is normalized to unity over mixing Ratio' needs further explanation. I went back to the Schwartz et al. (2013) paper for clarification and found the exact same statement. For me, to normalize each monthly histogram one would divide the population of each mixing ratio bin by the entire population or the population of the bin containing the mode or mean of the distribution. Assuming a somewhat Gaussian distribution, the normalization the mode or mean bin population would produce numbers near one and zero for the most and least populated bins (most and least probable in a PDF), respectively. This is how I interpret Figure 1 even though I don't understand "normalized to unity over mixing ratio" and the units on the color bar are  $\text{ppmv}^{-1}$ . What am I missing here?"

### Author's response and change to manuscript for referee's comment 1)

We have removed the old Figure 1 because it is unnecessary.

### Referee's Comment on Figure 1:

Figure 1 comment: "Also for Figure 1, the vertical lines are not "dashed" and the gray shading is too light, at least for my eyes."

### Author's response and change to manuscript for Figure 1:

We have removed the old Figure 1 of MLS data because it is redundant with other figures.

### Referee's Comment 2)

"The paper uses three vertical coordinates and doesn't tie them together very well. The introduction focuses on potential temperatures, everything pertaining to Figures 1-4 is discussed and shown in pressure coordinates, then Figures 5-7 are presented in altitude coordinates. Are the profiles in Figures 4-7 entirely in the lowermost stratosphere or do they extend into the overworld (or upper troposphere for that matter)? Profiles in Figures 4 extend from 150 to 50 hPa but in Figure 5a (same profiles) span 15.5 to 18.5 km. Are the axis ranges of these two Figures the same in terms of vertical span? I understand the need to discuss stratospheric layers in terms of potential temperature (introduction), but why can't everything else be presented uniformly using either pressure or altitude coordinates (or both together)? It would make the discussion and Figures much more intelligible."

### Author's response to comment 2:

To be consistent with previous literature on OT, the vertical coordinate of choice is altitude. We will change Figure 6 vertical coordinates to Altitude (left axis) and approximate Potential Temperature (right axis). Figures 4, 5, and 6 use the standard MLS 100-hPa product but we will modify each caption to 100 hPa (approximately 17 km altitude). The profiles in old figures 4-7 (revised figures 6-9) are mostly overworld stratosphere, with some lowermost stratosphere at the bottom of the profile (no upper tropospheric data are shown). This will be made clear by the revised y-axis of Figures 6, 7a, 8a, 9a.

Authors' Changes in Manuscript to comment 2:

New text in Abstract: "...were measured by the JPL Laser Hygrometer (JLH Mark2) at altitudes between 16.0 and 17.5 km (potential temperatures of approximately 380 K to 410 K)."

New text in new Figure 4 (old Figure 2) caption: "**Figure 4.** Distribution of Aura MLS v4.2 100-hPa H<sub>2</sub>O over CONUS (blue shaded box in insert), corresponding to approximately 17 km..."

New text in new Figure 5 (old Figure 3) caption: "**Figure 5.** Two-month mean map of Aura MLS v4.2 100-hPa H<sub>2</sub>O (color scale), corresponding to approximately 17 km altitude, with superimposed MERRA horizontal winds (arrows) for July-August 2013 during the SEAC<sup>4</sup>RS time period."

New Figure 6 and new Figure 6 caption:

**Figure 6.** Map and profiles of aircraft and satellite water vapor on 8 August 2013 over California (number 1 shown in dark blue) and Texas (number 2 shown in green). (a) Map of ER-2 aircraft flight track (solid colored trace) and nearly coincident Aura MLS geolocations (asterisks and lines). (b) ER-2 aircraft pressure profiles (solid colored trace) color-coded by dives and MLS times (horizontal lines). (c) Vertical profiles of water vapor from JLH Mark2 (dots), *in situ* with MLS averaging kernel (asterisks and lines), and MLS (circles and lines).

New revised y-axis of Figures 6, 7a, 8a, 9a (altitude and potential temperature) demonstrates that the plotted measurements are from the lowermost stratosphere and overworld stratosphere, not the troposphere. We have also replaced "UTLS" with "lower stratosphere" where appropriate in the text.

Referee's Comment 3):

[1] "Though the phrase 'enhanced water vapor' appears in the paper's title and is used frequently throughout the paper, it is never defined for the aircraft measurements. [2] Presumably there is a mixing ratio threshold used to identify air parcels with enhanced water vapor? The abstract may indirectly imply, likely incorrectly, that "enhanced" mixing ratios measured from aircraft are those >10 ppmv. [3] Adding to the mystery are the blue markers in panels (a) of Figures 5-7 that represent the "enhanced H<sub>2</sub>O region" but range well below 5 ppmv. What exactly is the threshold for "enhanced" water vapor measured from the aircraft? Why are there mixing ratios <5 ppmv in regions of enhanced water vapor? This is quite confusing and requires some important clarification in the paper."

Author's response to comment 3:

We agree with the referee that 'enhanced water vapor' should be presented more clearly.

[1] The phrase 'enhanced water vapor' will be defined (see below in author's changes).

[2] A mixing ratio threshold is identified as the mean plus 2 st. dev., which is 9.7 ppmv at 380-400 K, and 6.6 ppmv at 400-420 K (see below in author's changes).

[3] The referee is correct that panels (a) of Figures 5-7 are confusing, so these will be changed.

Author's changes in manuscript in response to comment 3:

[1] A definition, added to the paper at line 84 (new lines 107-108 in revised manuscript), is:

“Here we define ‘enhanced water vapor’ as mixing ratios greater than two standard deviations above the mean in situ measurement.” This is the threshold for ‘enhanced water vapor’ as measured from the aircraft.

[2] In the revised paper, we present a statistical analysis of the aircraft data, characterizing the mean, standard deviation and distribution of water vapor. The threshold for enhanced water is the campaign-wide mean plus 2 standard deviations. New text added at lines 108-110 in revised manuscript:

“For the overworld stratosphere in all 23 SEAC<sup>4</sup>RS flights, mean H<sub>2</sub>O for is  $6.7 \pm 1.5$  ppmv at 380-400 K (Figure 2), and  $5.0 \pm 0.8$  ppmv at 400-420 K (Figure 3). Thus the threshold for enhanced water vapor is 9.7 ppmv at 380-400 K, and 6.6 ppmv at 400-420 K.”

In the overworld stratosphere (potential temperature > 380 K), water vapor mixing ratios > 10 ppmv are unusual and thus “enhanced.” I should emphasize that the overworld stratosphere is typically drier than the lowermost stratosphere (350-380 K).

[3] The response to this comment is the same as the response to Figure 5 (see below in Referee’s Editorial Comments). We agree with the referee that this discussion is confusing, and have made changes to the manuscript. As described in lines 108-109, the threshold for ‘enhanced water vapor’ is mean + 2 sigma (from the combination of 23 aircraft flights) binned in two layers: 380-400 K and 400-420 K potential temperature. We observe these ‘enhanced water vapor’ events at 380-410 K (see Figure 1), so we call this layer the ‘enhanced water region.’ New text added at lines 112-113 in the revised manuscript:

“We define the ‘enhanced water region’ as the layer of the overworld stratosphere where these events have been observed, 380-410 K potential temperature corresponding to 16-17.5 km altitude.”

The blue points in (old) Figure 5 were confusing, so we removed them (see new Figures 7,8,9).

#### Referee’s Comment 4)

[1] “Is it appropriate to try to combine information from MLS and aircraft-based detections of water vapor in this paper when their thresholds are probably very different? Figure 3 shows only 13 instances where MLS retrievals at 100 hPa during Jul-Aug 2013 exceeded 8 ppmv. [2] Is this the threshold for MLS-detected “enhanced” water vapor? [3] Given the greatly different vertical and horizontal resolution of the MLS and aircraft measurements, how can the MLS findings be integrated with the aircraft-based results that follow? I don’t think they can. [4] What does a MLS retrieval of 8 ppmv with a 3-km averaging kernel width translate to for the in situ aircraft measurements? [5] Figures 1-3 contribute to only one conclusion drawn in this paper: that MLS retrievals at 100 hPa over the NAM region during Jul-Aug rarely exceed 8 ppmv. In my opinion that is a secondary (and already published) conclusion compared to the dominant conclusion of this paper that enhanced stratospheric water vapor measured over the NAM region during Jul-Aug 2013 can be traced back to convection-induced overshooting cloud tops.”

#### Author’s response to comment 4)

[1] We believe that it is appropriate to report information from MLS and aircraft because both satellite and aircraft show signals above background levels of water vapor in summer 2013, as shown in the revised Figure 6. We are not combining the MLS and aircraft datasets (although

Rodgers and Connor, 2003, showed mathematically how to do this). Instead, we are using both to describe the distribution of water vapor over the summer 2013 continental U.S.

[2] Yes, the referee is correct, the threshold for MLS-detected ‘enhanced water vapor’ is set at 8 ppmv. This is the same threshold that Schwartz et al. (2013) used to exclude the larger population of measurements at 6 to 8 ppmv water vapor that may have other sources.

[3] By using the histograms of overworld stratospheric water measured by aircraft (Figures 2 and 3) and MLS (Figure 4), we can conclude that these extreme events constitute only a percent or two of stratospheric observations. Furthermore, Figure 6 shows that both aircraft and MLS have significantly higher water vapor mixing ratios in regions with enhanced stratospheric water.

[4] We have calculated that an MLS retrieval of 8 ppmv with a 3-km averaging kernel width translates to 13 ppmv for *in situ* aircraft measurements. Three flights encountered greater than 13 ppmv in the overworld stratosphere, 12 Aug 2013, 27 Aug 2013 and 6 Sep 2013 (see Table 1).

[5] Each summer has different meteorology, and we wish to use a decade of MLS measurements to place 2013 in context. The Schwartz et al. (2013, Geophys. Res. Lett.) paper did not show data from the year 2013. There are three major results from the MLS figures that we want to retain in the paper: Summer 2013 was drier on average than the previous nine summers, 2004-2012 (Figure 4), the estimated frequency of H<sub>2</sub>O > 8ppmv was 0.9 percent (see below), and MLS clearly retrieved enhanced water vapor during the SEAC4RS time period (Figure 5). The author wishes to keep the MLS figures in the paper to demonstrate these points.

#### Author’s changes to manuscript for comment 4)

[1] revised Figure 6

[2] New text in Figure 4 caption: “The threshold for MLS-detected ‘enhanced water vapor’ (thick black vertical line) is set at 8 ppmv, same as Schwartz et al. (2013), to exclude the larger population of measurements at 6 to 8 ppmv water vapor that may have other sources.”

[3] We have introduced new histograms of JLH Mark2 water vapor (Figures 2 and 3), and updated the histogram of MLS water vapor (Figure 4) to integrate the aircraft and satellite findings.

[4] no change to manuscript for this point.

[5] revised Figures 4, 5, 6 and updated text in the Conclusions.

Referee’s Editorial Comments:

#### Referee’s Comment on (old) Line 58:

“please give the lowermost stratosphere a rough lower limit (in potential temperature) otherwise this implies it extends down to the surface. “Commonly” suggests these mechanisms are highly probably pathways for tropospheric water vapor to reach the stratosphere, which they are not.”

#### Author’s response to comment on (old) line 58:

The lowermost stratosphere extends from the tropopause (approx. 350 K over summer CONUS) to 380 K potential temperature.

We are unclear what the referee meant by “highly probable mechanisms for tropospheric water vapor to reach the stratosphere” because there are only three major mechanisms for tropospheric water vapor to reach the stratosphere:

- a) Transport through the tropical tropopause layer (TTL) followed by isentropic transport,
- b) Mixing across the tropopause,
- c) Overshooting tops.

Descent of middle stratospheric air brings very dry air to the lowermost stratosphere. The relatively high water mixing ratios and low ozone mixing ratios of the lowermost stratosphere indicate that water is transported from the troposphere to the lowermost stratosphere. Isentropic transport from the tropics is the dominant pathway for water into the lowermost stratosphere, with evidence from the seasonal cycle of water (e.g., Flury et al., 2013). What we mean at (old) line 58 is that high water mixing ratios in the midlatitude stratosphere are most likely caused by either mechanisms a, b, and/or c.

Author’s change to manuscript in response to (old) line 58:

We have modified the text at lines 58-63 in the revised manuscript:

“In contrast to water entry into the overworld stratosphere, water transport from the troposphere to the lowermost stratosphere ( $350\text{ K} < \theta < 380\text{ K}$  over summer CONUS) may occur through several different pathways. Poleward of the subtropical jet, water may be transported into the lowermost stratosphere through isentropic troposphere-stratosphere exchange (Holton et al., 1995) or through convective overshoot of the local tropopause (Dessler et al., 2007; Hanisco et al., 2007). Isentropic transport from the tropics is the dominant pathway for water into the lowermost stratosphere, with evidence from the seasonal cycle of water (e.g., Flury et al., 2013).”

Flury, T., Wu, D. L., and Read, W. G.: Variability in the speed of the Brewer-Dobson circulation as observed by Aura/MLS, *Atmos. Chem. Phys.*, 13, 4563–4575, [www.atmos-chem-phys.net/13/4563/2013/](http://www.atmos-chem-phys.net/13/4563/2013/), doi:10.5194/acp-13-4563-2013, 2013.

Referee’s Comment on (old) Line 62: “Please make it clear that ice (not elevated water) is transported into the stratosphere where it sublimates and produces “enhanced” water vapor mixing ratios.

Author’s response to (old) Line 62: The referee is correct.

Author’s change to the manuscript for (old) line 62:

We have modified the underlined text at lines 65-67 in the revised manuscript:

“Case studies have reported extreme events in which ice is transported to the overworld stratosphere and subsequently sublimates, but the amount of ice that is irreversibly injected into the stratosphere is poorly known.”

Referee’s Comment on (old) Line 63: “Here and elsewhere “stratospheric overworld” (defined in Line 45) has now become the “overworld stratosphere”.”

Author's response to (old) Line 63: Consistent with other publications, we will change the wording in line 45 and elsewhere from “stratospheric overworld” to “overworld stratosphere.”

Author's change to the manuscript for (old) line 63:

Throughout the revised manuscript, we now consistently use “overworld stratosphere”

Referee's Comment on (old) line 66: “Ice does not “bypass” the cold trap, it is unaffected by it.”

Author's response to (old) line 66: The referee is correct.

Author's change to manuscript for (old) line 66:

We have modified the underlined text at lines 69-70 in the revised manuscript:

“Ice injected directly into the stratosphere is unaffected by the cold trap in the vicinity of the tropopause (Ravishankara, 2012).”

Referee's Comment on (old) line 67: “Suggested paragraph break before “Paraphrasing” .”

Author's response to (old) line 67: This is a good suggestion.

Author's change to manuscript for (old) line 67:

We inserted a paragraph break at new line 72 with a new topic sentence:

“The subject of this paper is the role of convective overshooting tops in enhancing stratospheric water. Paraphrasing...”

Referee's Comment on (old) line 81: “are limited by their horizontal and vertical resolution in detecting fine-scale three-dimensional variations in water vapor ...”

Author's response to (old) line 81: the reviewer has a good suggestion.

Author's change to manuscript for (old) line 81:

We have modified the text at lines 86-87 in the revised manuscript to:

“Satellite measurements are limited by their horizontal and vertical resolution in detecting fine-scale three-dimensional variations in water vapor ...”

Referee's Comment on (old) line 101: “‘Instruments on the NASA ER-2’ – which instruments and what was measured that allows you to conclude that ‘the aircraft intercepted convectively-influenced air?’”

Author's response to (old) line 101: Only the hygrometers onboard the aircraft measured a convective signature (e.g., enhanced water vapor). Other tracers (including O<sub>3</sub>, CO<sub>2</sub>, CO, CH<sub>4</sub>) did not show a convective signature. We infer that lofted ice transported a disproportionate amount of condensed H<sub>2</sub>O relative to gas-phase tracers into the stratosphere.

Author's change to manuscript for (old) line 101:

We have modified the text at lines 117-120 in the revised manuscript to:

“Enhanced water vapor measured *in situ* by both the JLH Mark2 instrument and the Harvard Water Vapor instrument (J. B. Smith, pers. comm.) on the NASA ER-2 aircraft indicated that the aircraft intercepted convectively-influenced air. Other tracers measured on the aircraft did not change significantly in these plumes.”

Referee’s Comment on line 107: “‘measures daily global atmospheric profiles’ sounds like one gigantic profile is measured each day. How about ‘measures ~3500 profiles around the globe each day of atmospheric species ...’”

Author’s response to line 107: The reviewer has a good suggestion.

Author’s change to manuscript for (old) line 107:

We have changed the text at line 125 in the revised manuscript to:

“Aura MLS measures ~3500 profiles each day of water vapor and other atmospheric species (Livesey et al., 2016).”

Livesey, N. J., Read, W. G., Wagner, P. A., Froidevaux, L., Lambert, A., Manney, G. L., Millan Valle, L. F., Pumphrey, H. C., Santee, M. L., Schwartz, M. J., Wang, S., Fuller, R. A., Jarnot, R. F., Knosp, B. W., and Martinez, E.: Earth Observing System (EOS) Aura Microwave Limb Sounder (MLS) Version 4.2x Level 2 data quality and description document, Tech. Rep. JPL D-33509 Rev. B, Version 4.2x-2.0, Jet Propulsion Laboratory, California Institute of Technology, Pasadena, CA, available online at: <http://mls.jpl.nasa.gov/data/datadocs.php> (last access: May 9, 2016), 2016.

Referee’s comment on line 118: “Aren’t ‘the decadal histogram’ and ‘the previous multi-year MLS record’ the same thing in Figure 2? Don’t you want to compare and contrast the histogram of 2013 with the histogram of 10-year mean values? Figure 2 would be a great place to visually show (as a vertical line) the threshold for ‘enhanced’ MLS water vapor.”

Author’s response to line 118:

Yes, the referee is correct, the ‘decadal histogram’ and the ‘previous multi-year MLS record’ are the same. The purpose of new Figure 4 (old Figure 2) is to compare the histogram of July-August 2013 with the histogram of 9-summer mean values (also July-August).

Author’s change to manuscript for (old) line 118:

We have reworded this sentence at lines 135-137 in the revised manuscript:

“The histogram of Aura MLS water vapor in Figure 4 indicates that the July-August 2013 CONUS lower stratosphere was drier than the previous nine-summer MLS record (2004 to 2012).”

We have also added a vertical line to Figure 4 for the threshold for ‘enhanced’ MLS water vapor (8 ppmv). See Figure 4 in the revised manuscript and the new caption below:

**“Figure 4.** Distribution of Aura MLS v4.2 100-hPa H<sub>2</sub>O over CONUS (blue shaded box in insert), corresponding to approximately 17 km altitude. The two histograms for July-August 2013 (blue asterisks and trace) and the previous nine-summer MLS record, July-August 2004 through 2012

(red circles and trace) indicates that 2013 was drier than average. The 8-ppmv threshold for “enhanced” water vapor is shown by the thick black line.”

Referee’s comment on line 120: “You have the histograms so why say ‘rare’ when you can be quantitative?”

Author’s response on line 120: the referee has a good point here.

Author’s change to manuscript for (old) line 120:

We have inserted a new sentence at line 138-139 in the revised manuscript:

“From the MLS histogram, the frequency of 100-hPa H<sub>2</sub>O > 8ppmv was 0.9% of the observations in July-August 2013 in the blue shaded box.”

We also modified the sentence at line 275 in the final paragraph:

“The fraction of Aura MLS observations at 100 hPa with H<sub>2</sub>O greater than 8 ppmv is only 0.9% for July-August 2013.”

Referee’s comment on line 122: “At least 3 of the white circles in Figure 3 are near the west coast of Mexico, not Central America.”

Author’s response on line 122: The referee has a good point here about old Figure 3 (new Figure 5 in the revised manuscript).

Author’s change to manuscript for (old) line 122:

We have changed the text at lines 140-142 in the revised manuscript to:

“water greater than 8 ppmv was measured only nine times over North America (in the blue shaded box), three times near the west coast of Mexico, and once over the Caribbean Sea.”

Referee’s comment on line 146: “What is the spatial resolution (horizontal and vertical) of the convective storm information used to link ‘enhanced’ water vapor to overshooting tops? Later (Line 503) you say that the OT data are ‘high resolution’ but the spatial resolution is never described.”

Author’s response on line 146: The horizontal spatial resolution of the OT product is dependent on the underlying satellite imagery resolution, i.e., the size of the GOES IR pixel at any given spot. The size goes as you move further away from the subsatellite point. At subsatellite the pixel size is 4 km. At the junction between GOES East and GOES West, the pixel size is about 7 km in Montana, probably 6+ km in Mexico.

When the referee asks about the spatial resolution in the vertical dimension of the convective storm information, perhaps a more relevant question is: what is the accuracy of the OT altitude? This has been addressed in Griffin et al. (JAMC, 2016), who report that 75% of OT height retrievals are within 0.5 km of CloudSat OT height.

Author’s changes to manuscript for (old) line 146:

We have added text to lines 160-162 in the revised manuscript:

“For a description of the method, the reader is directed to Bedka et al. (2010). The horizontal spatial resolution of the OT product is dependent on the underlying satellite imagery resolution, i.e., the size of the GOES IR pixel, which is 7 km or less over the CONUS.”

And text to line 168-170 in the revised manuscript:

“Griffin et al. (2016) finds that 75% of OT height retrievals are within 0.5 km of CloudSat OT height, so we conservatively estimate the accuracy of the OT altitude to 0.5 km.”

Referee’s comment on line 156: “What was the time step interval for back trajectory calculations?”

Author’s response and change to manuscript for (old) line 156: To answer this question, we added the following text to lines 207-208 in the revised manuscript:

“..., and the trajectory time step interval was one hour.”

Referee’s comment on line 158: “How were these tolerances chosen? Do they have any relationship to the spatial resolution (horizontal and vertical) of the convective storm information?”

Author’s response and change to manuscript for (old) line 158: To answer this question, we added the following text to the end of the paragraph (lines 211-213 in the revised manuscript): “These tolerances were chosen primarily due to the resolution of the NCEP meteorology used to run the trajectories (1 deg x 1 deg) and also based on personal communication with Leonard Pfister.”

Referee’s comment on line 164: You already wrote about initializations (Line 153). This statement is again repeated in Line 180.

Author’s response on line 164: the referee has a good point and we will modify the text.

Author’s change to manuscript for (old) line 164:

The new text (removing initialization text) at line 218-219 in the revised manuscript is: “For each of these ER-2 flights, the back trajectories are presented along with the intersection of coincident OT.”

We also deleted the sentence at (old) line 180, and moved the rest of the paragraph to line 234 in the revised manuscript, after “Analysis of the 8 August 2013 case is shown in Figure 7.”

Referee’s comment on line 169: It would be beneficial to include the lats/lons of these sites.

Author’s response and changes to the manuscript for (old) line 169: we have modified the text at line 222-223 in the revised manuscript to:

“Palmdale, California (34.6 °N, 118.1 °W), to Ellington Field, Houston, Texas (29.6 °N, 95.2 °W).”

Referee's comment on line 173: Same comment as for Line 58.

Author's response to line 173: we will give a lower limit to the lowermost stratosphere: 350 K potential temperature.

Author's change to manuscript for (old) line 173:

At line 226-227 in the revised manuscript we have changed the text to:

“(350 K <  $\theta$  < 380 K)”

Referee's comment on line 182: This information is already in the Figure Captions.

Author's response on line 182: the referee has a good point but we feel that some text is required here to guide the reader through the plots in new Figure 7 (old Figure 5).

Author's change to manuscript for (old) line 182:

Starting at line 234 in the revised manuscript, we slightly modified the text to:

“Analysis of the 8 August 2013 case is shown in Figure 7. For clarity only some example trajectories (a subset of our analysis) are shown. These are displayed as thin blue traces in panels (b) and (c). The initial water vapor mixing ratios of the example trajectories are shown as red squares in panels (a). The intersections of the example trajectories with coincident OT are shown as red squares in panels (b) and (c). All overshooting convective tops within +/-3 hours of the red squares are shown by green symbols in panels (b) and (c).”

Referee's comment on line 184: In Figures 5-7, panels (b) and (c), the green markers show “near coincidences” (within the tolerances listed in Line 158) between back trajectories and OTs, while red squares show “coincidences”. What are the criteria for “coincidences”?

Author's response on line 184: We thank the referee for catching this typo. The description in the original text doesn't quite match what's on the figure. The red symbols are where there were coincidences for the specific example trajectories plotted in light blue. The green symbols show all overshooting convective locations within +/- 3 hours of the red points, **not** related to where any of the trajectories went (see modified text above).

We changed the text in (old) Figure captions 5, 6 and 7 to remove "nearly coincident" since the only coincidence for green markers is in time. That doesn't really qualify as nearly coincident. The reason to show all the green symbols is to give an indication of how robust the coincidences are. For instance, the mass of green points north of Texas on Aug. 8 indicates there were a lot of overshoots there and the coincidences should be robust for the trajectories that went through that region. The two coincidences in Arizona are among only a small cluster of overshoots and so this is not as robust a coincidence.

The criteria for coincidence (red markers) is, as described in Section 3.2:

“+/-0.25 degrees latitude and longitude, +/-3 hours, +/-0.5 km in altitude.”

Author's change to manuscript for (old) line 184:

We removed "nearly coincident" from the captions for (old) Figures 5, 6 and 7 (new Figures 7, 8, 9 in the revised manuscript).

Referee's comment on line 191: In Figure 5b there are many green markers in western Mexico, so why is this location not listed?

Author's response on line 191: This was confusing because the original text did not properly describe the green markers. As described above, green markers are not coincident. Only the red markers are coincident in space and time, so we only describe the locations of the red markers.

Referee's comment on line 198: In Figure 5d there are many red markers depicting transit times >6 days, but here you claim domination by transit times of "two to five days".

Author's response on line 198: Thank you to the referee for catching this typo. Please note old Figure 5d is now Figure 7d in the revised manuscript.

Author's change to manuscript for (old) line 198:

We changed the text at line 248 in the revised manuscript from "two to five days earlier than" to "within seven days prior to".

Referee's comment on line 205: TX, OK and AR are in the "South Central" U.S.

Author's response and change to manuscript for (old) line 205: The referee is correct. At line 254 in the revised manuscript we have replaced "Central" with "South Central".

Referee's comment on line 216: Define MCC as mesoscale convective complex.

Author's response and change to manuscript for (old) line 216: This is a good point. The term is only used once, so at line 265 in the revised manuscript, we have replaced "MCC" with "mesoscale convective complex".

Referee's comment on line 227: Earlier you stated that back trajectories were initialized for every measurement of enhanced water vapor. Now, "Example" infers that this was done only for a subset. Did "all" (Line 228) of the back trajectories connect to OTs? Really? All?

Author's response on line 227: The referee has an excellent point here. Not all of the back trajectories connect to OTs, although a significant fraction of trajectories do connect to OTs (see Figure 10 and below in "changes to the manuscript"). Back trajectories were initialized at every 1-sec time stamp along the flight track in the "enhanced water vapor layer" (16-17.5 km altitude).

Author's changes to the manuscript in response to (old) line 227:

To characterize the fraction of trajectories that intersect OT, we introduce a new Figure 10 and new text at lines 280-282 in the Conclusions:

“For all the back trajectories in this analysis, the fraction that connect to OT within the previous seven days ranges from 30% to 70% (Figure 10).”

Also, we have deleted the old text “Example air parcel back-trajectories were initialized at the locations and time of enhanced water. All of the back-trajectories connect these air parcels to convective OT one to seven days prior to aircraft intercept.”

and added the following text at lines 276-278 of the revised manuscript:

“Back trajectories initialized at every 1-sec time stamp along the aircraft flight track at 16 to 17.5 km connect the sampled air parcels to convective OT within seven days prior to the flight.”

Referee’s comment on line 230: Figure 9b shows there were influences from storm systems in South Central Canada as well.

Author’s response and changes for (old) line 230: The referee is correct. We have added to line 280 of the revised manuscript: “and South Central Canada.”

Referee’s comment on line 235: “leaving behind” should be “producing”

Author’s response and change for (old) line 235: The referee is correct. We have changed the text at lines 286-287 of the revised manuscript to:

“... producing water vapor mixing ratios elevated 10 ppmv or more above background levels.”

Referee’s comment on line 238: “propel water” gives the wrong impression while “loft ice” is more accurate.

Author’s response and changes to (old) line 238: The referee is correct. At line 289 in the revised manuscript we have changed “propel water” to “loft ice”.

Referee’s comment on line 239: “the enriched delta-D isotopic signature” needs a bit more explanation, including a mention of the isotope itself, HDO.

Author’s response and changes to (old) line 239: The referee has a good point. We have modified the text starting at line 290 in the revised manuscript.

“Further evidence of ice is provided by water isotopologues. Evaporation and condensation are fractionating processes for isotopologues, especially HDO relative to H<sub>2</sub>O (e.g., Craig, 1961; Dansgaard, 1964). Condensation preferentially concentrates the heavier HDO isotopologue, so lofted ice is relatively enriched in HDO/H<sub>2</sub>O compared to gas phase (e.g., Webster and Heymsfield, 2003, and references therein). Ice sublimation is supported by the enriched HDO/H<sub>2</sub>O isotopic signature observed by the ACE satellite over summertime North America (Randel et al., 2010).”

New references:

Craig, H.: Isotopic Variations in Meteoric Waters, *Science*, 133, 1702-3, doi: 10.1126/science.133.3465.1702, 1961.

Dansgaard, W.: Stable isotopes in precipitation, *Tellus*, 16, 436-68, 1964.

Referee's comment on line 246: "The water is almost certainly injected in the ice phase" needs support. I suggest you combined this paragraph with all or some of the previous paragraph that provides such support.

Author's response and changes to (old) line 246: Done. We have merged this paragraph (line 299 of revised manuscript) with the previous paragraph.

Referee's Comment on Line 252: "from a long (200 km) path through the atmosphere" also needs to include information about the vertical resolution. The qualitative statement "may be enhanced even more" is the basis for my argument that the MLS and aircraft results cannot be meaningfully integrated together in this paper.

Author's response and change to manuscript in response to (old) Line 252:

The simple answer about vertical resolution is ~3 km vertical resolution for MLS water in the lower stratosphere. We have replaced the text at (old) line 252 to the following new text at line 311 in the revised manuscript:

"Limb measurements from Aura MLS come from a ~200 km path through the atmosphere with ~3 km vertical resolution in the lower stratosphere (Livesey et al., 2016). The aircraft profiles of water vapor are very similar on ascent and descent profiling (Figure 6c), which allows us to estimate the horizontal length of these features as greater than 180 km, and a vertical thickness of ~0.5 km. This size is sufficiently large that the MLS retrieval is sensitive to enhanced water, as shown in Figure 6c."

Referee's Comment on Line 254: what percent of the 10 years of MLS observations show enhanced water?

Author's response and changes to paper for Line 254: our answer is in the revised paper starting at line 304 (for better flow):

"The fraction of Aura MLS observations at 100 hPa with H<sub>2</sub>O greater than 8 ppmv is only 0.9% for July-August 2013. In comparison, Schwartz et al. (2013) reports that, for the nine-year record 2004-2012, July and August had 1.4% and 3.2% of observations exceed 8 ppmv, respectively."

Referee's Comment on Line 261: Which "monsoon region"?

Author's response and change to manuscript for Line 261: Randel et al. (2015) addresses the North American Monsoon (NAM) region. We have changed the text in the revised lined 322 to: "NAM region."

Referee's Comment on old Figure 2 Caption: "ten year mean for 2004 through 2013."

Author's response on old Figure 2 Caption: We decided to compare 2013 with the previous nine-summer record, 2004 through 2012.

Author's changes to manuscript for old Figure 2 Caption (new Figure 4 caption):

Old Figure 2 has been updated to new Figure 4 in the revised manuscript, and the caption changed to:

"Distribution of Aura MLS v4.2 100-hPa H<sub>2</sub>O over CONUS (blue shaded box in insert), corresponding to approximately 17 km altitude. The two histograms for July-August 2013 (blue asterisks and trace) and the previous nine-summer MLS record, July-August 2004 through 2012 (red circles and trace) indicates that 2013 was drier than average. The threshold for MLS-detected 'enhanced water vapor' (thick black vertical line) is set at 8 ppmv, same as Schwartz et al. (2013), to exclude the larger population of measurements at 6 to 8 ppmv water vapor that may have other sources."

Referee's Comment on old Figure 3 Caption: "Average Aura MLS 100-hPa"

Author's response and change to old Figure 3 Caption (new Figure 5): we changed the new Figure 5 Caption to "Two-month mean map of Aura MLS v4.2 100-hPa..."

Referee's Comment on old Figure 4: "[1] Colored markers are not "retrievals" from the aircraft, they are the actual aircraft measurements. [2] Why do multiple aircraft profiles produce only one profile convolved with the MLS averaging kernels? Without strongly magnifying this Figure I can't tell the difference between the MLS profiles and the convolved aircraft profile. I suggest omitting the convolved aircraft profile in each panel. It does show that the averaging kernels smooth the aircraft profiles, but isn't that exactly what one would expect anyway?"

[3] Also, the black asterisks showing MLS retrieval locations on flight track maps are difficult to distinguish from black map lines. Perhaps larger gray symbols "x" or "+" would stand out more?"

[4] And the "line" mentioned in the caption, is this the horizontal line in each "Flight Altitude" (should be "Pressure") vs UTC hour panel indicating the time range of measurements shown in the profiles? [5] This Figure would be an ideal place to visually show (as a vertical line in each profile panel) the threshold for aircraft "enhanced" water vapor."

Author's response on old Figure 4: These are great points by the referee. We will implement changes as listed below.

Author's changes to old Figure 4 (Figure 6 in revised manuscript):

[1] We have changed the figure 6 caption from "water vapor retrievals from aircraft (color), aircraft with MLS averaging kernel (asterisk and lines)" to "Vertical profiles of *in situ* water vapor measurements from JLH Mark2 (dots) and MLS retrievals of water vapor (circles and lines)."

[2] As the referee recommended, we have omitted the convolved aircraft profile for improved clarity in Figure 6c (previously, multiple aircraft profiles were combined to produce one profile convolved with the MLS averaging kernels).

[3] We have changed the MLS retrieval symbols in Figure 6a to colored asterisks for clarity.

[4] Yes, the MLS measurement times are signified by the colored horizontal lines in Figure 6b. The Pressure vs UTC hour panel is now altitude vs time (Figure 6b), properly labeled “Altitude”, with new caption “MLS times (horizontal lines)”.

[5] To address the referee’s comment, we have added text to the Figure 6c caption:

“Some measurements exceed the threshold for enhanced water vapor of 8 ppmv for Aura MLS (after Schwartz et al., 2013), and the campaign-wide mean plus 2 st. dev. for JLH Mark 2, 9.7 ppmv at 380-400 K and 6.6 ppmv at 400-420 K.”

Referee’s Comment on Figure 5: These comments apply to each of Figures 5-7: In panels (a), the captions claim the blue markers denote “enhanced water measurements” (which range below 5 ppmv) while in the panel (a) legends the blue markers are said to represent the “Enhanced H<sub>2</sub>O region”, which must be something quite different from “enhanced water vapor” measurements. This distinction needs to be clarified in the paper by defining exactly what is meant by the terms “enhanced water measurements” and “enhanced H<sub>2</sub>O region”.

Author’s response and change to (old) Figures 5-7: We agree with the referee that this discussion is confusing, and have made changes to the manuscript. As described in lines 108-109, the threshold for ‘enhanced water vapor’ is mean + 2 sigma (from the combination of 23 aircraft flights) binned in two layers: 380-400 K and 400-420 K potential temperature. We observe these ‘enhanced water vapor’ events at 380-410 K (see Figure 1), so we call this layer the ‘enhanced water region.’

New text added at lines 112-113 in the revised manuscript:

“We define the ‘enhanced water region’ as the layer of the overworld stratosphere where these events have been observed, 380-410 K potential temperature corresponding to 16-17.5 km altitude.”

The blue points in (old) Figure 5 were confusing, so we removed them (see new Figures 7,8,9).

Authors' response to anonymous referee #2 on "Enhanced Stratospheric Water Vapor over the Summertime Continental United States and the Role of Overshooting Convection" by R. L. Herman et al., ACP-2016-1065.

We would like to thank the referee #2 for detailed comments (shown in quotations below). The individual points are addressed by the authors below:

Referee's General Comment:

Review of "Enhanced Stratospheric Water Vapor over the Summertime Continental United States and the Role of Overshooting Convection" by Herman et al.

"This paper presents direct airborne measurements of water injection into the lowermost stratosphere over the continental United States by convective overshooting tops and relates these to individual overshooting events through trajectory analysis. The study is generally well written, however, the overall result and conclusion is somewhat weak. I would recommend this paper for publication only after major revisions, for which I give suggestions below."

Author's response to general comment: we have addressed all of the referee's points below in the major and minor comments. Both the text and some figures have been modified in response to the referee's comments.

Referee's Major comments:

The observations themselves are not new and a number of previous studies have clearly indicated that overshooting convection may transport water ice into the stratosphere, where it evaporates and increases the stratospheric water vapor concentration. The novelty of this study is that it links observed water vapor enhancements to possible overshooting top events through trajectory analysis. This result, while new, is not very surprising and leaves the paper with a rather insignificant result. [1] The paper would benefit strongly from a discussion of the significance of this result and a much enhanced statistical analysis using their entire observational set. The authors indicated that they have many more observations during this campaign but chose to show only three examples. The authors might want to use their entire data set and increase their statistical analysis. [2] Their only statistical argument is at the end of the discussion, where they use only MLS data to state, that the impact is small. However, their own data (Figure 4) shows nicely, that MLS misses the highest concentrations due to its strong vertical averaging, which will heavily skew the result. Since the water vapor enhancements seem present on a very large scale, it would be good to see the entire data set for this campaign. The authors could then attempt to make a statistical analysis on how well they can relate these enhancements to OT events, what their temporal distribution may have been, and if there could be some preferred regions. [3] In the past water vapor instruments onboard the high altitude aircraft have shown significant disagreements. The authors state, that the other instruments show similar results. It would be good to actually show these, which would support the confidence in the observations themselves.

Authors' Response and Change to manuscript in response to Referee's Major Comment [1]:

We agree with the referee that the paper would benefit strongly from a discussion of the significance and statistical analysis using the entire dataset. The significance is that the "enhanced" water measurements can be traced, for the first time, back to storm clusters with identified OT events in several common geographical areas. In the revised manuscript, three new figures (Figures 1, 2 and 3) characterize the distribution of stratospheric water vapor on all SEAC<sup>4</sup>RS flights. Out of 23 flights over the continental United States (CONUS), eleven showed enhanced water vapor. Details of these eleven flights are shown in the new Table 1, and discussed in the updated Section 2.1.

Authors' Response and Change to manuscript in response to Referee's Major Comment [2]:

Aura MLS has a significant signal in H<sub>2</sub>O from lower stratospheric enhanced water events. The threshold for MLS is 8 ppmv (Schwartz et al., 2013) to exclude points at 6-8 ppmv that may have other sources of water. The revised figure 6 (old figure 4) has been made clearer to demonstrate that the 'enhanced' water over the South Central U.S. (point 2 in this figure) is well above typical mixing ratios both for the aircraft data and the MLS satellite measurements.

Authors' Response to Referee's Major Comment [3]:

During SEAC<sup>4</sup>RS, the agreement between the two water vapor instruments on the ER-2 (JLH Mark2 and Harvard Water Vapor) is within +/-10% for stratospheric water. This is consistent with the AquaVIT laboratory intercomparison (Fahey et al., 2014). The Harvard data are not presented here because they will appear in a companion paper by J. Smith et al. In the past, other water vapor instruments had different biases, but we assert that those instruments would also show enhanced water well above their measured mean.

Author's Change to manuscript in response to Referee's Major Comment [3]:

New text added in revised manuscript at line 120-121:

"During SEAC<sup>4</sup>RS, the agreement between the two water vapor instruments on the ER-2 is within +/-10% for stratospheric water. This is consistent with the AquaVIT laboratory intercomparison (Fahey et al., 2014)."

New Reference added to revised paper:

Fahey, D. W., Gao, R.-S., Möhler, O., Saathoff, H., Schiller, C., Ebert, V., Krämer, M., Peter, T., Amarouche, N., Avallone, L. M., Bauer, R., Bozóki, Z., Christensen, L. E., Davis, S. M., Durrý, G., Dyroff, C., Herman, R. L., Hunsmann, S., Khaykin, S., Mackrodt, P., Meyer, J., Smith, J. B., Spelten, N., Troy, R. F., Vömel, H., Wagner, S., and Weinhold, F. G.: The AquaVIT-1 Intercomparison of Atmospheric Water Vapor Measurement Techniques, *Atmos. Meas. Tech.*, 7, 3177-3213, doi:10.5194/amt-7-3177-2014, 2014.

Minor comments:

Referee's minor comment 1:

"The manuscript should try to stick to one vertical coordinate and add other vertical coordinates only as additional information, e.g '90 hPa (370 K)'. Figure 4 uses pressure as vertical coordinate for consistency with MLS. Therefore, this could be the vertical coordinate system of choice. The profile figures may add approximate potential temperature as additional vertical axis for reference."

Author's Response and Changes in Manuscript in response to comment 1:

The referee has a good point here and the figures will be modified. To be consistent with previous literature on OT, the vertical coordinate of choice is altitude. We have changed Figure 6 (old Figure 4) vertical coordinates to "Altitude" (left axis) and "Approx. Pot. Temperature" (right axis). MLS Figures 4, 5, 6 (old Figures 1, 2 and 3) use the standard MLS 100-hPa product but we will modify each caption to "100 hPa (approximately 17 km altitude)..." In the Conclusions, we replaced "between 160 and 80 hPa" with "16 to 17.5 km altitude." (note, "160 hPa" was a typo and should have read "115 hPa").

Referee's minor comment 2:

"Most data shown in Figure 4 repeat between panels a-c. This figure could be combined into one panel with MLS data color coded roughly following the aircraft data."

Authors' Response and Change to manuscript in response to minor comment 2: Figure 6 (Old Figure 4) has been remade, with panels combined, and easier to read.

Referee's minor comment 3:

The use of green dots in Figures 5-7 is confusing. Panels c seem to indicate coincidences with relaxed conditions, whereas panels b seem to indicate all overshooting top events in the given time frame to show convective regions. This should be clarified.

Author's response to minor comment 3:

We agree with the referee that this was presented in a confusing manner. The description in the original text doesn't quite match what's on the figure. In panels b and c, the red symbols are where there were coincidences for the specific example trajectories plotted in light blue. Likewise, in panels b and c, the green symbols show all overshooting convective locations within +/- 3 hours of the red points, **not** related to where any of the trajectories went.

Author's change to manuscript in response to minor comment 3:

We removed "nearly coincident" from the manuscript since the only coincidence for green markers is in time. That doesn't really qualify as nearly coincident. The reason to show all the green symbols is to give an indication of how robust the coincidences are. For instance, the mass of green points north of Texas on 8 Aug 2013 indicates there were a lot of overshoots there and the coincidences should be robust for the trajectories that went through that region. The two coincidences in Arizona are among only a small cluster of overshoots and so this is not as robust a coincidence.

Referee's minor comment 4:

There are several references to "stratospheric background levels". [1] How were these background levels defined for this purpose? Are the profiles west of the Rocky Mountains considered "background" or did the authors use something else to define what the background is for this purpose? If they used the West Coast profiles, then they should briefly discuss the meteorology and exclude that these are more typical high latitude profiles. Could it be that the "background" is not as low as the authors assume?

[2] There is obviously a large uncertainty in the detection and assignment of OT events. It would be good if the authors discussed how this uncertainty impacts their identification of possibly source events. [3] What is the lifetime of a typical overshooting top? [4] How many are likely to be missed by the OT detection algorithm? [5] Especially on the events that are closer to the observations, can the authors identify individual events that are best candidates?

Authors' Responses and Changes to manuscript in response to minor comment 4 [1]:

The mean water vapor for all flights is 5.0 +/- 0.8 ppmv at 400 K < potential temperature < 420 K (new Figure 3), but this mean is biased higher by high outliers of H<sub>2</sub>O. In comparison, Figure 6 (and previously published work) show that background stratospheric water for MLS is typically 3 to 5 ppmv.

New text at line 112-113:

"The majority of measurements have background water mixing ratios characteristic of the overworld stratosphere, 4 to 6 ppmv."

Authors' Responses and Changes to manuscript in response to minor comment 4 [2]:

Uncertainty "in the detection and assignment of OT events" is discussed below in point 4 [4], 'How many are likely to be missed by the OT detection algorithm.'

New text added to Section 3:

"Given uncertainties in back trajectories, GOES under-sampling, and that many OTs can be located in close proximity to one another, we are not able to make a direct connection between an individual OT and a stratospheric water vapor plume observed a day or more later. Rather, our analysis identifies a cluster of storms that are the best candidates for generating ice that sublimates into enhanced water vapor plumes sampled by the ER-2."

Authors' Responses to minor comment 4 [3]:

The lifetime of a typical overshooting top can range from less than 10 minutes to greater than one hour.

Authors' change to manuscript in response to minor comment 4 [3]:

New text added to section 3:

"The ability of GOES-East and GOES-West to observe an OT depends on its lifetime. OTs are transient events with lifetimes typically less than 30 mins but can exceed an hour in well-organized storms such as mesoscale convective systems and supercell storms (Bedka et al.

2015; Solomon et al., 2016, and references therein). Animations such as the following show the variability of OTs sampled by GOES at 1-min resolution.

Infrared wavelength animation:

[http://cimss.ssec.wisc.edu/goes/srsor2015/800x800\\_AGOES14\\_B4\\_MS\\_AL\\_IR\\_animated\\_2015\\_222\\_191500\\_182\\_2015223\\_131500\\_182\\_IR4AVHRR2.mp4](http://cimss.ssec.wisc.edu/goes/srsor2015/800x800_AGOES14_B4_MS_AL_IR_animated_2015_222_191500_182_2015223_131500_182_IR4AVHRR2.mp4)

Visible wavelength animation:

[http://cimss.ssec.wisc.edu/goes/blog/wp-content/uploads/2015/08/150811\\_goes14\\_visible\\_srsor\\_MS\\_mcs\\_anim.gif](http://cimss.ssec.wisc.edu/goes/blog/wp-content/uploads/2015/08/150811_goes14_visible_srsor_MS_mcs_anim.gif)

It is clear that some OTs are quite persistent and are both prominent and detectable in IR imagery, but the majority of OTs in these particular animations are short lived (< 10 mins). Within these OTs, strong convective updrafts can transport ice to 16-18 km altitude where turbulent processes such as gravity wave breaking mix tropospheric and stratospheric air (e.g., Mullendore et al., 2009, 2005; Wang 2003; Homeyer et al. 2017), enabling detrainment of ice and stratospheric hydration.”

#### Authors’ Response and change to manuscript for minor comment 4 [4]:

New text added to section 3:

“Bedka et al. (2010) showed that the OT detection algorithm has a false positive rate of 4.2% to 38.8%, depending on the size of the overshooting and algorithm settings. As noted above, OTs are transient and can evolve quite rapidly. The storm top characteristics and evolution we see in the GOES data featured in this paper only capture a subset of the storm lifetimes, even if we were to have a 100% OT detection rate, due to the 15 min resolution of the GOES imager. In addition, relatively coarse GOES spatial resolution (up to 7 km over northern latitudes of the US) can cause the Bedka et al. (2010) method to miss some small diameter and/or weak OT regions. We would be able to better map storm updraft tracks using data at 1-minute frequency like that shown by Bedka et al. (2015), but this data is not available over broad geographic domains required for our analysis. Given uncertainties in back trajectories, GOES under-sampling, and that many OTs can be located in close proximity to one another, we are not able to make a direct connection between an individual OT and a stratospheric water vapor plume observed a day or more later. Rather, our analysis identifies a cluster of storms that are the best candidates for generating ice that sublimates into enhanced water vapor plumes sampled by the ER-2.”

Although not added to the text, we note that GOES-13 did observe at 7.5 min intervals during some days of the SEAC4RS campaign when severe storms were forecasted over the U.S. but this only represents a small subset of the data analyzed in this paper.

#### New References added to the revised manuscript:

Bedka, K., Wang, C., Rogers, R., Carey, L., Feltz, W., and Kanak, J.: Examining deep convective cloud evolution using total lightning, WSR-88D, and GOES-14 super rapid scan datasets. *Wea. Forecasting*, 30, 571–590, doi:10.1175/WAF-D-14-00062.1, 2015.

Solomon, D. L., Bowman, K. P., and Homeyer, C. R.: Tropopause-Penetrating Convection from Three-Dimensional Gridded NEXRAD Data, *J. Appl. Met. Climat.*, 55, 465-78, DOI:10.1175/JAMC-D-15-0190.1, 2016.

Mullendore, G. L., Durran, D. R., and Holton, J. R.: Cross-tropopause tracer transport in midlatitude convection, *J. Geophys. Res.*, 110, D06113, doi:10.1029/2004JD005059, 2005.

Mullendore, G. L., Homann, A. J., Bevers, K., and Schumacher, C.: Radar reflectivity as a proxy for convective mass transport, *J. Geophys. Res.*, 114, D16103, doi:10.1029/2008JD011431, 2009.

Liu, N., and Liu, C.: Global distribution of deep convection reaching tropopause in 1 year GPM observations, *J. Geophys. Res. Atmos.*, 121, doi:10.1002/2015JD024430, 2016.

Homeyer, C., McAuliffe, J., and Bedka, K. M.: On the Development of Above-Anvil Cirrus Plumes in Extratropical Convection, *J. Atmos. Sci.*, In Press, available online at: <http://journals.ametsoc.org/doi/abs/10.1175/JAS-D-16-0269.1>

Author's response to comment 4 [5]: No, we cannot identify individual OT events for each back trajectory. There is considerable uncertainty in the detection and assignment of OT events, but the ensemble of trajectories repeatedly show coincidences with OT in specific storm clusters, especially for the 27 August 2013 case.

Author's changes to text in response to comment 4 [5]:

New text added in Section 3:

"Given uncertainties in back trajectories, GOES under-sampling, and that many OTs can be located in close proximity to one another, we are not able to make a direct connection between an individual OT and a stratospheric water vapor plume observed a day or more later. Rather, our analysis identifies a cluster of storms that are the best candidates for generating ice that sublimates into enhanced water vapor plumes sampled by the ER-2."

Referee's Comment on Lines 118-119: better: '...was drier than the 10 year MLS record ...'

Authors' Response and change to manuscript: We changed the old lines 118-119 to reworded lines 135-137 in the revised manuscript (note that old Figure 2 is now Figure 4): "The histogram of Aura MLS water vapor in Figure 4 indicates that the July-August 2013 CONUS lower stratosphere was drier than the previous nine-summer MLS record (2004 to 2012)."

Referee's Comment on Lines 129-130: better '...the storm systems from which they may have originated, it is necessary...'

Authors' Response and change to manuscript: We agree with the referee, and changed the old lines 129-130 to the suggested text (lines 149-150 in the revised manuscript): '...the storm systems from which they may have originated, it is necessary...'

1 **Title**

2

3 **Enhanced Stratospheric Water Vapor over the Summertime**  
4 **Continental United States and the Role of Overshooting Convection**

5 Robert L. Herman<sup>1</sup>, Eric A. Ray<sup>2</sup>, Karen H. Rosenlof<sup>2</sup>, Kristopher M. Bedka<sup>3</sup>, Michael J.  
6 Schwartz<sup>1</sup>, William G. Read<sup>1</sup>, Robert F. Troy<sup>1</sup>, Keith Chin<sup>1</sup>, Lance E. Christensen<sup>1</sup>, Dejian Fu<sup>1</sup>,  
7 Robert A. Stachnik<sup>1</sup>, T. Paul Bui<sup>4</sup>, Jonathan M. Dean-Day<sup>5</sup>

8 <sup>1</sup>Jet Propulsion Laboratory, California Institute of Technology, Pasadena, California, USA.

9 <sup>2</sup>National Oceanic and Atmospheric Administration (NOAA) Earth System Research Laboratory (ESRL) Chemical  
10 Sciences Division, Boulder, Colorado, USA.

11 <sup>3</sup>NASA Langley Research Center, Hampton, Virginia, USA.

12 <sup>4</sup>NASA Ames Research Center, Moffett Field, California, USA.

13 <sup>5</sup>Bay Area Environmental Research Institute, Sonoma, California, USA.

14 *Correspondence to:* R. L. Herman (Robert.L.Herman@jpl.nasa.gov)

15 **Abstract**

16 The NASA ER-2 aircraft sampled the lower stratosphere over North America during the NASA Studies of  
17 Emissions and Atmospheric Composition, Clouds and Climate Coupling by Regional Surveys (SEAC<sup>4</sup>RS) field  
18 mission. This study reports observations of convectively-influenced air parcels with enhanced water vapor in the  
19 overworld stratosphere over the summertime continental United States, and investigates in detail three case studies.  
20 Water vapor mixing ratios greater than 10 ppmv, much higher than the background 4 to 6 ppmv of the overworld  
21 stratosphere, were measured by the JPL Laser Hygrometer (JLH Mark2) at altitudes between 16.0 and 17.5 km  
22 (potential temperatures of approximately 380 K to 410 K). Overshooting cloud tops (OT) are identified from a  
23 SEAC<sup>4</sup>RS OT detection product based on satellite infrared window channel brightness temperature gradients.  
24 Through trajectory analysis, we make the connection between these *in situ* water measurements and OT. Back  
25 trajectory analysis ties enhanced water to OT one to seven days prior to the intercept by the aircraft. The trajectory  
26 paths are dominated by the North American Monsoon (NAM) anticyclonic circulation. This connection suggests that  
27 ice is convectively transported to the overworld stratosphere in OT events and subsequently sublimated; such events  
28 may irreversibly enhance stratospheric water vapor in the summer over Mexico and the United States. Regional  
29 context is provided by water observations from the Aura Microwave Limb Sounder (MLS).

30

31 **Keywords**

32 Convection, overshoot, atmospheric water, stratosphere-troposphere exchange

33

34 **Copyright Statement**

35 Copyright 2017. All rights reserved.

36 **1. Introduction**

37 Water plays a predominant role in the radiative balance of the Earth’s atmosphere, both in the gas phase as the  
38 Earth’s primary greenhouse gas and in condensed phases in cloud and aerosol. Despite its low abundance, upper  
39 tropospheric and lower stratospheric (UTLS) water vapor is critically important in controlling outgoing long-wave  
40 radiation, and quantifying UTLS water vapor and its controlling processes is critical for climate characterization and  
41 prediction. Climate models are sensitive to changes in stratospheric water (Shindell, 2001) and clouds (Boucher et  
42 al., 2013). Increases in UTLS water are associated with warming at the surface on the decadal scale (Solomon et al.,  
43 2010). As the dominant source of hydroxyl radicals, UTLS water also plays an important role in control of UTLS  
44 ozone (Shindell, 2001; Kirk-Davidoff et al., 1999).

45  
46 The overworld stratosphere, the altitude region with potential temperature  $\theta$  greater than 380 K (Holton et al. 1995),  
47 is extremely dry, with typical mixing ratios of 3—6 parts per million by volume (ppmv). The importance of low  
48 temperatures at the tropical tropopause acting as a “cold trap” to prevent tropospheric water from entering the  
49 stratosphere has been recognized since Brewer (1949). Tropospheric air slowly ascends through the tropical  
50 tropopause layer (TTL) as part of the hemispheric-scale Brewer-Dobson circulation. In the TTL, air passes through  
51 extremely cold regions where water vapor condenses in situ to form cirrus ice, and then the cirrus slowly falls due to  
52 sedimentation (e.g., Jensen et al., 2013). Additional condensation and sedimentation are thought to be associated  
53 with convection and large-scale waves (e.g., Voemel et al., 2002). The amount of water that enters the stratosphere  
54 is largely a function of the coldest temperature a parcel trajectory encounters. This typically occurs in the tropics,  
55 and the coldest temperature is typically near the tropical tropopause. The saturation mixing ratio at the cold point  
56 tropopause thereby sets the entry value of water vapor.

57  
58 In contrast to water entry into the overworld stratosphere, water transport from the troposphere to the lowermost  
59 stratosphere ( $350\text{ K} < \theta < 380\text{ K}$  over summer CONUS) may occur through several different pathways. Poleward of  
60 the subtropical jet, water may be transported into the lowermost stratosphere through isentropic troposphere-  
61 stratosphere exchange (Holton et al., 1995) or through convective overshoot of the local tropopause (Dessler et al.,  
62 2007; Hanisco et al., 2007). Isentropic transport from the tropics is the dominant pathway for water into the  
63 lowermost stratosphere, with evidence from the seasonal cycle of lower stratospheric water (e.g., Flury et al., 2013).  
64 How important sublimation of ice from convective overshoot is for hydrating the stratosphere is a topic of ongoing  
65 debate (e.g., Randel et al., 2015; Wang, 2003). Case studies have reported extreme events in which ice is transported  
66 to the overworld stratosphere and subsequently sublimates, but the amount of ice that is irreversibly injected into the  
67 stratosphere is poorly known. Airborne measurements have demonstrated that convective injection occurs both in  
68 the tropics (Webster and Heymsfield, 2003; Corti et al., 2008; Sayres et al., 2010; Sargent et al., 2014) and at mid-  
69 latitudes (Hanisco et al., 2007; Anderson et al., 2012). Ice injected directly into the stratosphere is unaffected by the  
70 cold trap in the vicinity of the tropopause (Ravishankara, 2012).

71  
72 The subject of this paper is the role of convective overshooting tops in enhancing stratospheric water. Paraphrasing  
73 Bedka et al. (2010), a convective overshooting top (OT) is a protrusion above a cumulonimbus anvil due to strong

74 updrafts above the equilibrium level. Early observations of OT include photographs of OT in the stratosphere from a  
75 U-2 aircraft (Roach 1967). Recent observations of elevated water mixing ratios in the summer overworld  
76 stratosphere by aircraft (Anderson et al., 2012) and the Aura Microwave Limb Sounder (MLS) (Schwartz et al.,  
77 2013) suggest that ice injection into the overworld stratosphere by OT, while rare, occurs in three predominant  
78 regions during the summer season. These three regions are the Asian Monsoon region, the South American  
79 continent, and – the focus of this study - the North American Monsoon (NAM) region (Schwartz et al., 2013).

80

81 The NASA ER-2 aircraft sampled the summer stratospheric NAM region during the NASA Studies of Emissions  
82 and Atmospheric Composition, Clouds and Climate Coupling by Regional Surveys (SEAC<sup>4</sup>RS) field mission (Toon  
83 et al., 2016). One of the primary goals of this multi-aircraft mission was to address the question: do deep convective  
84 cloud systems locally inject water vapor and other chemicals into the overworld stratosphere over the continental  
85 United States (CONUS)? It is challenging for space- and ground-based techniques to detect enhanced water vapor  
86 injected into the stratosphere by OT. Satellite measurements are limited by their horizontal and vertical resolution in  
87 detecting fine-scale three-dimensional variations in water vapor, while ground-based measurements are confined to  
88 sampling at fixed locations. In contrast, airborne *in situ* stratospheric measurements of water have an advantage  
89 because the aircraft can be routed to a specific location, altitude, date and time. Modelers can predict whether air  
90 parcels are likely to have convective influence, and aircraft flight paths are planned to intercept those air parcels.  
91 The purpose of this paper is to report three new case studies of enhanced water vapor in the overworld stratosphere  
92 during the NASA SEAC<sup>4</sup>RS field mission, and to connect these observations to deep convective OT over the North  
93 American continent.

94

## 95 **2. Observations**

### 96 **2.1 Aircraft**

97 The airborne *in situ* water vapor measurements reported here are from the Jet Propulsion Laboratory Laser  
98 Hygrometer Mark2 (JLH Mark2), a tunable laser spectrometer with an open-path cell external to the aircraft  
99 fuselage (May, 1998). Water vapor is reported at 1 Hz (10% accuracy), although the time response of the open-path  
100 cell is much faster than this because the instrument is sampling the free-stream airflow. This instrument has a  
101 redesigned optomechanical structure for greater optical stability, and was first flown in this configuration on the  
102 NASA ER-2 high-altitude aircraft during the SEAC<sup>4</sup>RS field mission. Pressure and temperature, provided by the  
103 Meteorological Measurement System (MMS) (Scott et al., 1990), are used in the data processing to calculate water  
104 vapor mixing ratios from spectra, as described in May (1998).

105

106 During SEAC<sup>4</sup>RS, nine aircraft flights targeted air parcels with recent convective influence (see Table 3 of Toon et  
107 al., 2016). Figure 1 shows the combined vertical profiles of JLH Mark2 water vapor from all 23 SEAC<sup>4</sup>RS flights.  
108 Outliers with high water vapor mixing ratios are the focus on this study. Enhanced water vapor was measured on  
109 eleven flights (Table 1). Here we define ‘enhanced water vapor’ as mixing ratios greater than two standard  
110 deviations above the mean *in situ* measurement. For the overworld stratosphere in all 23 SEAC<sup>4</sup>RS flights, mean

111 H<sub>2</sub>O for is  $6.7 \pm 1.5$  ppmv at 380-400 K (Figure 2), and  $5.0 \pm 0.8$  ppmv at 400-420 K (Figure 3). Thus the threshold for  
112 enhanced water vapor is 9.7 ppmv at 380-400 K, and 6.6 ppmv at 400-420 K. The majority of measurements have  
113 background water mixing ratios characteristic of the overworld stratosphere, 4 to 6 ppmv. In the overworld  
114 stratosphere (potential temperature greater than 380 K), Figure 1 shows enhanced water vapor at potential  
115 temperatures up to approximately 410 K (17.5 km altitude). We define the ‘enhanced water region’ as the layer of  
116 the overworld stratosphere where these events have been observed, 380-410 K potential temperature corresponding  
117 to 16-17.5 km altitude. Enhanced water vapor measured *in situ* by both the JLH Mark2 instrument (Figure 1) and the  
118 Harvard Water Vapor instrument (J. B. Smith, pers. comm.) on the NASA ER-2 aircraft indicated that the aircraft  
119 intercepted convectively-influenced air. Other tracers measured on the aircraft did not change significantly in these  
120 plumes. For the SEAC<sup>4</sup>RS flights, the agreement between these two water vapor instruments is within +/-10% for  
121 stratospheric water. This is consistent with the AquaVIT laboratory intercomparison (Fahey et al., 2014). The largest  
122 enhancements were observed on three flights that are described in detail in Sect. 4.

123

## 124 2.2 Aura MLS

125 Aura MLS measures ~3500 profiles each day of water vapor and other atmospheric species (Livesey et al., 2016).  
126 While the aircraft samples *in situ* water in a thin trajectory through the atmosphere, Aura MLS provides a larger  
127 scale context. Expanding on the analysis of Schwartz et al. (2013), Aura MLS observations of stratospheric water  
128 vapor are presented here for the SEAC<sup>4</sup>RS time period of summer 2013. Aura MLS H<sub>2</sub>O has 0.4 ppmv precision at  
129 100 hPa for individual profile measurements, with spatial representativeness of 200 km along line-of-sight  
130 (Schwartz et al., 2013). Results shown here use MLS version 4.2 data, but are not significantly different from the  
131 previous version 3.3. MLS observations over CONUS are at ~14:10 local time (ascending orbit) and ~1:20 local time  
132 (descending orbit), with successive swaths separated by ~1650 km. Vertical resolution of the water vapor product is  
133 ~3 km in the lower stratosphere (Livesey et al., 2016).

134

135 Aura MLS shows a seasonal maximum in water vapor over CONUS in July and August. The histogram of Aura  
136 MLS water vapor in Figure 4 indicates that the July-August 2013 CONUS lower stratosphere was drier than the  
137 previous nine-summer MLS record (2004 to 2012). Nevertheless, enhanced lower stratospheric water vapor was  
138 observed by MLS in 2013 as rare but detectable events. From the MLS histogram, the frequency of 100-hPa H<sub>2</sub>O >  
139 8ppmv was 0.9% of the observations in July-August 2013 in the blue shaded box. Figure 5 shows that, out of all  
140 MLS 100-hPa water vapor retrievals over the two-month period July to August 2013, water greater than 8 ppmv was  
141 measured only nine times over North America (in the blue shaded box), three times near the west coast of Mexico,  
142 and once over the Caribbean Sea.

143

## 144 3. Analysis

145 Here we briefly describe the analytical technique used to determine whether back trajectories from the aircraft  
146 location intersect OT as identified by a satellite OT data product.

147

148 **3.1 Detection of overshooting tops**

149 In order to link the stratospheric water vapor encountered by the aircraft to the storm systems from which they may  
150 have originated, it is necessary to have a comprehensive continental scale catalog of deep convection. Geostationary  
151 Operational Environmental Satellite (GOES) infrared imagery is used to assemble a catalog of OTs throughout the  
152 U.S. and offshore waters. This catalog was acquired from the NASA LaRC Airborne Science Data From  
153 Atmospheric Composition data archive (<http://www-air.larc.nasa.gov/cgi-bin/ArcView/seac4rs>). Because OTs are  
154 correlated with storm intensity, the OT product was primarily developed to benefit the aviation community for more  
155 accurate turbulence prediction, as well as the general public for earlier severe storm warnings. However, the product  
156 is also ideally suited for identifying storm systems that can moisten the stratosphere.

157  
158 Infrared brightness temperatures are used to detect cloud top temperature anomalies within thunderstorm anvils. OT  
159 candidates are colder than the mean surrounding anvil, with the temperature difference indicative of both the  
160 strength of the convective updraft and the depth of penetration. For a description of the method, the reader is  
161 directed to Bedka et al. (2010). The horizontal spatial resolution of the OT product is dependent on the underlying  
162 satellite imagery resolution, i.e., the size of the GOES IR pixel, which is 7 km or less over the CONUS. Additional  
163 validation of OTs requires comparison with the Global Forecast System (GFS) Numerical Weather Prediction  
164 (NWP) model tropopause temperature. The maximum OT cloud height was derived based on knowledge of the 1)  
165 OT-anvil temperature difference, 2) the anvil cloud height based on a match of the anvil mean temperature near to  
166 the OT and the GFS NWP temperature profile, and 3) a temperature lapse rate within the UTLS region based on a  
167 GOES-derived OT-anvil temperature difference and NASA CloudSat OT-anvil height difference for a sample of  
168 direct CloudSat OT overpasses (Griffin et al., 2016). Griffin et al. (2016) finds that 75% of OT height retrievals are  
169 within 0.5 km of CloudSat OT height, so we conservatively estimate the accuracy of the OT altitude to 0.5 km. For  
170 SEAC<sup>4</sup>RS, every available GOES-East and GOES-West scan (typically 15 min resolution) was processed for the  
171 full duration of the mission, even for the non-flight days, yielding a detailed and comprehensive picture of the  
172 location, timing, and depth of penetration of convective storms over the entire CONUS. The output files include the  
173 OT coordinates, time, overshooting intensity in degrees K – which is related to the temperature difference between  
174 the OT and the anvil – and an estimate of maximum cloud height for OT pixels in meters.

175  
176 The ability of GOES-East and GOES-West to observe an OT depends on its lifetime. OTs are transient events with  
177 lifetimes typically less than 30 minutes but can exceed an hour in well-organized storms such as mesoscale  
178 convective systems and supercell storms (Bedka et al. 2015; Solomon et al., 2016, and references therein).

179 Animations such as the following show the variability of OTs sampled by GOES at 1-min resolution,  
180 Infrared wavelength animation:

181 [http://cimss.ssec.wisc.edu/goes/srsor2015/800x800\\_AGOES14\\_B4\\_MS\\_AL\\_IR\\_animated\\_2015222\\_191500\\_182\\_2015223\\_131500\\_182\\_IR4AVHRR2.mp4](http://cimss.ssec.wisc.edu/goes/srsor2015/800x800_AGOES14_B4_MS_AL_IR_animated_2015222_191500_182_2015223_131500_182_IR4AVHRR2.mp4)

183 Visible wavelength animation:

184 [http://cimss.ssec.wisc.edu/goes/blog/wp-content/uploads/2015/08/150811\\_goes14\\_visible\\_srsor\\_MS\\_mcs\\_anim.gif](http://cimss.ssec.wisc.edu/goes/blog/wp-content/uploads/2015/08/150811_goes14_visible_srsor_MS_mcs_anim.gif)

185 It is clear that some OTs are quite persistent and are both prominent and detectable in IR imagery, but the majority  
186 of OTs in these particular animations are short lived (< 10 minutes). Within these OTs, strong convective updrafts  
187 can transport ice to 16-18 km altitude where turbulent processes such as gravity wave breaking mix tropospheric and  
188 stratospheric air (e.g., Mullendore et al., 2009, 2005; Wang 2003; Homeyer et al. 2017), enabling detrainment of ice  
189 and stratospheric hydration.

190  
191 Bedka et al. (2010) showed that the OT detection algorithm has a false positive rate of 4.2% to 38.8%, depending  
192 on the size of the overshooting and algorithm settings. As noted above, OTs are transient and can evolve quite  
193 rapidly. The storm top characteristics and evolution we see in the GOES data featured in this paper only capture a  
194 subset of the storm lifetimes, even if we were to have a 100% OT detection rate, due to the 15 min resolution of the  
195 GOES imager. In addition, relatively coarse GOES spatial resolution (up to 7 km over northern latitudes of the US)  
196 can cause the Bedka et al. (2010) method to miss some small diameter and/or weak OT regions. We would be able  
197 to better map storm updraft tracks using data at 1-minute frequency like that shown by Bedka et al. (2015), but this  
198 data is not available over broad geographic domains required for our analysis. Given uncertainties in back  
199 trajectories, GOES under-sampling, and that many OTs can be located in close proximity to one another, we are not  
200 able to make a direct connection between an individual OT and a stratospheric water vapor plume observed a day or  
201 more later. Rather, our analysis identifies a cluster of storms that are the best candidates for generating ice that  
202 sublimates into enhanced water vapor plumes sampled by the ER-2.

203

### 204 **3.2 Back trajectory modeling**

205 Back trajectories were run from each flight profile where enhanced water vapor was measured to determine whether  
206 the sampled air was convectively influenced. The trajectories were run with the FLEXPART model (Stohl et al.,  
207 2005) using NCEP Climate Forecast System version 2 (CFSv2) meteorology (Saha et al., 2014), and the trajectory  
208 time step interval was one hour. Trajectories were initialized every second along the flight track profiles and run  
209 backward for seven days. A sampled air parcel was determined to be convectively influenced if the back trajectory  
210 from that parcel intercepted an OT region. The tolerances for a trajectory to be considered to have intercepted an OT  
211 cloud were +/-0.25 degrees latitude and longitude, +/-3 hours, +/-0.5 km in altitude. These tolerances were chosen  
212 primarily due to the resolution of the NCEP meteorology used to run the trajectories (1 deg x 1 deg) and also based  
213 on personal communication with Leonard Pfister.

214

## 215 **4. Case Studies**

216 In this section, we highlight three NASA ER-2 flights where elevated stratospheric water was observed by JLH  
217 Mark2. These dates are 8, 16 and 27 August 2013. Similar results are seen from other hygrometers on the NASA  
218 ER-2 aircraft (J. B. Smith, pers. comm.). For each of these ER-2 flights, the back trajectories are presented along  
219 with the intersection of coincident OT. The cases are described below.

220

### 221 **4.1 First case: 8 August 2013**

222 Figure 6 shows details of the 8 August 2013 ER-2 aircraft flight. This flight was the transit flight from Palmdale,  
223 California (34.6 °N, 118.1 °W), to Ellington Field, Houston, Texas (29.6 °N, 95.2 °W). In addition to sending the  
224 NASA ER-2 aircraft to the destination base, the science goal of this flight was to profile the North American  
225 Monsoon region with five profiles plus the aircraft ascent and final descent. This flight shows a dramatic transition  
226 from west to east of background stratospheric water to enhanced water. In the lowermost stratosphere ( $350 \text{ K} < \theta <$   
227  $380 \text{ K}$ ), water can be highly variable, but at 90 hPa it is generally unusual to observe water vapor greater than 6  
228 ppmv. As shown in Figure 6c, there is a gradient in water vapor from west to east: 4.0 to 4.4 ppmv at 90 hPa (17  
229 km) over the west coast of CONUS (black and blue points), and greater than 10 ppmv at 90 hPa over Texas (green  
230 points). Simultaneous Aura MLS retrievals also demonstrate a west-to-east water vapor gradient on this day (lines  
231 and filled circles in Figure 6c). Both JLH Mark2 and Aura MLS water vapor exceed the thresholds for enhanced  
232 water vapor.

233  
234 Analysis of the 8 August 2013 case is shown in Figure 7. For clarity only some example trajectories (a subset of our  
235 analysis) are shown. These are displayed as thin blue traces in panels (b) and (c). The intersections of the example  
236 trajectories with coincident OT are shown as red squares in panels (b) and (c). All overshooting convective tops  
237 within +/-3 hours of the red squares are shown by green symbols in panels (b) and (c). Back trajectories from the  
238 flight track follow the anticyclonic NAM circulation over Western Mexico, Great Plains and Mississippi Valley  
239 (Figure 7b). Every one of the example back trajectories intersects OT, as shown by red symbols in Figure 7b. For  
240 this flight, coincidences with overshooting convection are dominated by overshooting clouds over the Mississippi  
241 Valley and Great Plains. All overshooting convection within the tolerances prescribed (see Sect. 3.2) for the back  
242 trajectories are shown by the green symbols in Figure 7b and 5c. Figure 7c demonstrates the range of altitudes  
243 reached by the coincident overshooting convection and how many convective overshooting cells were coincident.  
244 The high resolution of the convective overshooting data meant that there could be multiple coincident convective  
245 overshooting cells for a single location on a back trajectory. It is significant that some of the green overshooting  
246 cells are higher altitude than the red coincident points, suggesting that overshooting air parcels descended slightly  
247 before mixing with the surrounding air. Figure 7d indicates the source of enhanced water was dominated by  
248 overshooting clouds within seven days prior to intercept by the aircraft.

#### 249 250 **4.2 Second case: 16 August 2013**

251 The NASA ER-2 flight of 16 August 2013 was designed to survey the North American Monsoon in a triangular  
252 flight path from Houston, Texas, to the Imperial Valley in Southern California, to Southeastern Colorado and back  
253 to Texas. The NASA ER-2 aircraft performed six dives, encountering enhanced stratospheric water at 16 to 17 km  
254 altitude (Figure 8a). As shown in Figure 8b, back trajectories intersect overshooting tops over the South Central U.S.  
255 (Texas, Oklahoma, Arkansas) and also over the Sierra Madre Occidental mountain range on the west coast of  
256 Mexico. This case is an example of the classic North American Monsoon circulation with a moisture source over the  
257 Sierra Madre Occidental. Anticyclonic transport carried the moisture north from Mexico, and counter-clockwise  
258 around the high pressure (Figure 8b). The altitude range of the convective overshoot is typically 16 to 17 km

259 altitude, as shown in Figure 8c. The time between OT and intercept by the aircraft ranges from two to seven days  
260 (Figure 8d).

261

### 262 **4.3 Third case: 27 August 2013**

263 The 27 August 2013 flight performed six dives to sample the North American Monsoon. Stratospheric water was  
264 enhanced to 15 to 20 ppmv in altitudes ranging from 16.0 to 17.5 km (Figure 9a). The ER-2 aircraft intercepted  
265 highly enhanced stratospheric water from a mesoscale convective complex over the Upper Midwest, which had  
266 overshooting tops over Northern Minnesota and Northern Wisconsin (Toon et al., 2016), as shown in Figure 9b.  
267 Figure 9c shows an abundance of OT above 17 km (green). Generally speaking, the OT appear at higher altitudes in  
268 the northern CONUS/southern Canada than in the Central CONUS. Figure 9d shows that the air masses were  
269 sampled *in situ* by the ER-2 aircraft over Illinois and Indiana one to two days after the intense storm. As is a  
270 common theme for all these experiment days, a portion of the back-trajectories also trace back to overshooting tops  
271 over the Sierra Madre Occidental one week prior.

272

## 273 **5. Conclusions**

274 In this paper we have examined *in situ* measurements of stratospheric water by JLH Mark2 on the ER-2 aircraft  
275 during the SEAC<sup>4</sup>RS field mission. With JLH Mark2 data, enhanced H<sub>2</sub>O above background mixing ratios was  
276 frequently encountered in the overworld stratosphere between 16 and 17.5 km altitude. Back trajectories initialized  
277 initialized at every 1-sec time stamp along the aircraft flight track at 16 to 17.5 km connect the sampled air parcels  
278 to convective OT within seven days prior to the flight. The trajectory modeling indicates that the identified OT are  
279 associated with larger storm systems over the Central U.S. (Figure 7), deep convection over the Sierra Madre  
280 Occidental (Figure 8), and deep convection over the Upper Midwest U.S. and South Central Canada (Figure 9). For  
281 all the back trajectories in this analysis, the fraction that connect to OT within the previous seven days ranges from  
282 30% to 70% (Figure 10).

283

284 The concentrations of enhanced water and the connection to OT suggests a mechanism for moistening the CONUS  
285 lower stratosphere: ice is irreversibly injected into the overworld stratosphere by the most intense convective tops.  
286 The temperatures of the CONUS lower stratosphere are sufficiently warm to sublimate the ice, producing water  
287 vapor mixing ratios elevated 10 ppmv or more above background levels. The summertime CONUS has a high  
288 frequency of thunderstorms with sufficient energy to transport ice to the upper troposphere (Koshak et al., 2015, and  
289 references therein). On rare occasion, these storms have sufficient energy to loft ice through the tropopause and into  
290 the stratosphere. Further evidence of ice is provided by water isotopologues. Evaporation and condensation are  
291 fractionating processes for isotopologues, especially HDO relative to H<sub>2</sub>O (e.g., Craig, 1961; Dansgaard, 1964).  
292 Condensation preferentially concentrates the heavier HDO isotopologue, so lofted ice is relatively enriched in  
293 HDO/H<sub>2</sub>O compared to gas phase (e.g., Webster and Heymsfield, 2003, and references therein). Ice sublimation is  
294 supported by the enriched HDO/H<sub>2</sub>O isotopic signature observed by the ACE satellite over summertime North  
295 America (Randel et al., 2010). Cross-tropopause transport is a consequence of turbulent mixing at cloud top,

296 possibly enhanced by the existence of breaking gravity waves often occurring near overshooting cloud tops. (Wang,  
297 2003). This study addresses a primary goal of the SEAC<sup>4</sup>RS field mission (Toon et al., 2016), answering  
298 affirmatively the science question: “Do deep convective cloud systems locally inject water vapor and other  
299 chemicals into the overworld stratosphere over the CONUS?” This water is almost certainly injected in the ice  
300 phase and subsequently sublimated in the relatively warm stratosphere over CONUS, leading to irreversible  
301 hydration. From this study, we conclude that the depth of injection was typically 16 to 17.5 km altitude for these  
302 particular summertime events.

303  
304 Satellite retrievals of water vapor from Aura MLS provide a larger-scale context. The fraction of Aura MLS  
305 observations at 100 hPa (approximately 17 km altitude) with H<sub>2</sub>O greater than the 8 ppmv threshold is 0.9% for  
306 July-August 2013. In comparison, Schwartz et al. (2013) reports that, for the nine-year record 2004-2012, July and  
307 August had 1.4% and 3.2% of observations exceed 8 ppmv, respectively. This reinforces the conclusion of Randel et  
308 al. (2015) that OT play a minor role in the mid-latitude stratospheric water budget. At the 100-hPa level in the lower  
309 stratosphere, the year 2013 was slightly drier than the average of 2004-2012 summers (Figure 4). Despite the  
310 relatively dry conditions of summer 2013, there was sufficient enhanced water to be clearly observed in the Aura  
311 MLS retrievals (Figures 4, 5, 6). Limb measurements from Aura MLS come from a ~200 km path through the  
312 atmosphere with ~3 km vertical resolution in the lower stratosphere (Livesey et al., 2016). The aircraft profiles of  
313 water vapor are very similar on ascent and descent profiling (Figure 6c), which allows us to estimate the horizontal  
314 length of these features as greater than 180 km, and a vertical thickness of ~0.5 km. This size is sufficiently large  
315 that the MLS retrieval is sensitive to enhanced water, as shown in Figure 6c.

316  
317 *In situ* measurements probe on a small-scale air parcels that can be connected to OT that inject ice and, to a lesser  
318 extent, trace gases to the stratosphere (e.g., Ray et al., 2004; Hanisco et al., 2007; Jost et al, 2004). In contrast,  
319 modeling studies tend to focus on large-scale processes. Dessler et al. (2002) and Corti et al. (2008) concluded that  
320 OT are a significant source of water vapor in the mid-latitude lower stratosphere. In contrast, Randel et al. (2015)  
321 used Aura MLS observations to conclude that circulation plays a larger role than OT in controlling mid-latitude  
322 stratospheric water vapor in the NAM monsoon region. Our study shows clear evidence of observable perturbations  
323 to stratospheric water vapor on ER-2 aircraft flights that targeted convectively-influenced air during SEAC<sup>4</sup>RS. In  
324 future work, we plan more detailed back trajectory analysis of air parcels over summertime North America to better  
325 understand the transport of ice and water in the lower stratosphere.

326 **Code Availability**

327 n/a

328

329 **Data Availability**

330 Data discussed in this manuscript are publically available. The NASA aircraft data are available through the  
331 following digital object identifier (DOI): SEAC4RS DOI 10.5067/Aircraft/SEAC4RS/Aerosol-TraceGas-Cloud.

332

333 **Appendices: none**

334

335 **Supplement link: none**

336

337 **Team List:**

338 Robert L. Herman<sup>1</sup>, Eric A. Ray<sup>2</sup>, Karen H. Rosenlof<sup>2</sup>, Kristopher M. Bedka<sup>3</sup>, Michael J.  
339 Schwartz<sup>1</sup>, William G. Read<sup>1</sup>, Robert F. Troy<sup>1</sup>, Keith Chin<sup>1</sup>, Lance E. Christensen<sup>1</sup>, Dejian Fu<sup>1</sup>,  
340 Robert A. Stachnik<sup>1</sup>, T. Paul Bui<sup>4</sup>, Jonathan M. Dean-Day<sup>5</sup>

341 <sup>1</sup>Jet Propulsion Laboratory, California Institute of Technology, Pasadena, California, USA.

342 <sup>2</sup>National Oceanic and Atmospheric Administration (NOAA) Earth System Research Laboratory (ESRL) Chemical  
343 Sciences Division, Boulder, Colorado, USA.

344 <sup>3</sup>NASA Langley Research Center, Hampton, Virginia, USA.

345 <sup>4</sup>NASA Ames Research Center, Moffett Field, California, USA.

346 <sup>5</sup>Bay Area Environmental Research Institute, Sonoma, California, USA.

347

348 **Author Contribution**

349 Robert Herman prepared the manuscript with contributions from all coauthors and was responsible for all aspects of  
350 the JLH Mark2 as principal investigator. Eric Ray and Karen Rosenlof provided trajectory calculations and  
351 interpretation. Kristopher Bedka provided an overshooting top data product and interpretation. Robert Troy, Robert  
352 Stachnik and Keith Chin operated the JLH Mark2 instrument in the field and downloaded data. Robert Stachnik,  
353 Dejian Fu, Lance Christensen and Keith Chin also developed software components for the JLH Mark2 instrument.  
354 Michael Schwartz and William Read provided Aura MLS data and statistical analysis. T. Paul Bui and Jonathan  
355 Dean-Day measured pressure and temperature with the MMS instrument and provided data.

356

357 **Competing interests:**

358 The authors declare that they have no conflict of interest.

359

360 **Disclaimer**

361

362 **Acknowledgements**

363 We thank Jose Landeros and Dave Naticic for providing technical support in the laboratory and field, and the aircraft  
364 crew and flight planners for making these measurements possible. The JLH Mark2 team is supported by the NASA  
365 Upper Atmosphere Research Program and Radiation Sciences Program. Part of this research was performed at JPL,  
366 California Institute of Technology, under a contract with NASA.

367 **References**

- 368 Anderson, J. G., Wilmouth, D. M., Smith, J. B., and Sayres, D. S.: UV Dosage Levels in Summer: Increased Risk of  
369 Ozone Loss from Convectively Injected Water Vapor, *Science*, 337(6096), 835-839, 2012.
- 370 Bedka, K. M., Brunner, J., Dworak, R., Feltz, W., Otkin, J., and Greenwald, T.: Objective satellite-based  
371 overshooting top detection using infrared window channel brightness temperature gradients. *J. Appl. Meteor.*  
372 *Climatol.*, **49**, 181-202, 2010.
- 373 Bedka, K. M., Wang, C., Rogers, R., Carey, L., Feltz, W., and Kanak, J.: Examining deep convective cloud  
374 evolution using total lightning, WSR-88D, and GOES-14 super rapid scan datasets, *Wea. Forecasting*, **30**,  
375 571–590, doi:10.1175/WAF-D-14-00062.1, 2015.
- 376 Boucher, O., Randall, D., Artaxo, P., Bretherton, C., Feingold, G., Forster, P., Kerminen, V.-M., Kondo, Y., Liao,  
377 H., Lohmann, U., Rasch, P., Satheesh, S. K., Sherwood, S., Stevens B., and Zhang, X. Y.: Clouds and  
378 Aerosols. In: *Climate Change 2013: The Physical Science Basis. Contribution of Working Group I to the*  
379 *Fifth Assessment Report of the Intergovernmental Panel on Climate Change* (Stocker, T. F., Qin, D., Plattner,  
380 G.-K., Tignor, M., Allen, S. K., Boschung, J., Nauels, A., Xia, Y., Bex, V., and Midgley, P. M. (eds.)),  
381 Cambridge University Press, Cambridge, United Kingdom and New York, NY, USA, 2013.
- 382 Brewer, A. W.: Evidence for a world circulation provided by the measurements of helium and water vapor  
383 distribution in the stratosphere, *Q. J. Roy. Met. Soc.*, **75**, 351-63, 1949.
- 384 Corti, T., Luo, B. P., De Reus, M., Brunner, D., Cairo, F., Mahoney, M. J., Martucci, G., Matthey, R., Mitev, V.,  
385 Dos Santos, F. H., Schiller, C., Shur, G., Sitnikov, N. M., Spelten, N., Voessing, H. J., Borrmann, S., and  
386 Peter, T.: Unprecedented evidence for deep convection hydrating the tropical stratosphere, *Geophys. Res.*  
387 *Lett.*, **35**, L10810, doi:10.1029/2008GL033641, 2008.
- 388 Craig, H.: Isotopic Variations in Meteoric Waters, *Science*, **133**, 1702-3, doi: 10.1126/science.133.3465.1702, 1961.
- 389 Dansgaard, W.: Stable isotopes in precipitation, *Tellus*, **16**, 436-68, 1964.
- 390 Dessler, A. E., Hanisco, T. F., and Fueglistaler, S.: Effects of convective ice lofting on H<sub>2</sub>O and HDO in the tropical  
391 tropopause layer, *J. Geophys. Res.*, **112**, doi:10.1029/2007JD008609, 2007.
- 392 Fahey, D. W., Gao, R.-S., Möhler, O., Saathoff, H., Schiller, C., Ebert, V., Krämer, M., Peter, T., Amarouche, N.,  
393 Avallone, L. M., Bauer, R., Bozóki, Z., Christensen, L. E., Davis, S. M., Durr, G., Dyroff, C., Herman, R.  
394 L., Hunsmann, S., Khaykin, S., Mackrodt, P., Meyer, J., Smith, J. B., Spelten, N., Troy, R. F., Vömel, H.,  
395 Wagner, S., and Weinhold, F. G.: The AquaVIT-1 Intercomparison of Atmospheric Water Vapor  
396 Measurement Techniques, *Atmos. Meas. Tech.*, **7**, 3177-3213, doi:10.5194/amt-7-3177-2014, 2014.
- 397 Flury, T., Wu, D. L., and Read, W. G.: Variability in the speed of the Brewer-Dobson circulation as observed by  
398 Aura/MLS, *Atmos. Chem. Phys.*, **13**, 4563–4575, www.atmos-chem-phys.net/13/4563/2013/  
399 doi:10.5194/acp-13-4563-2013, 2013.
- 400 Griffin, S. M., Velden, C. S., and Bedka, K. M.: A method for calculating the height of overshooting convective  
401 cloud tops using satellite-based IR imager and CloudSat cloud profiling radar observations, *J. Appl. Met. and*  
402 *Clim.*, **55**, 479-491, DOI: <http://dx.doi.org/10.1175/JAMC-D-15-0170.1>, 2016.

403 Hanisco, T. F., Moyer, E. J., Weinstock, E. M., St. Clair, J. M., Sayres, D. S., Smith, J. B., Lockwood, R.,  
404 Anderson, J. G., Dessler, A. E., Keutsch, F. N., Spackman, J. R., Read, W. G., and Bui, T. P.: Observations of  
405 deep convective influence on stratospheric water vapor and its isotopic composition, *Geophys. Res. Lett.*, *34*,  
406 L04814, doi:10.1029/2006GL027899, 2007.

407 Holton, J.R., P.H. Haynes, A.R. Douglass, R.B. Rood, and L. Pfister: Stratosphere–troposphere exchange. *Rev.*  
408 *Geophys.*, *33*(4), 403–439, 1995.

409 Homeyer, C., McAuliffe, J., and Bedka, K. M.: On the Development of Above-Anvil Cirrus Plumes in Extratropical  
410 Convection, *J. Atmos. Sci.*, In Press, available online at: [http://journals.ametsoc.org/doi/abs/10.1175/JAS-D-](http://journals.ametsoc.org/doi/abs/10.1175/JAS-D-16-0269.1)  
411 [16-0269.1](http://journals.ametsoc.org/doi/abs/10.1175/JAS-D-16-0269.1)

412 Jensen, E. J., Diskin, G., Lawson, R. P., Lance, S., Bui, T. P., Hlavka, D., McGill, M., Pfister, L., Toon, O. B., and  
413 Gao, R., Ice nucleation and dehydration in the Tropical Tropopause Layer, *Proc. Nat. Acad. Sci.*, *110*(6),  
414 2041–2046, 2013.

415 Jensen, E. J., Smith, J. B., Pfister, L., Pittman, J. V., Weinstock, E. M., Sayres, D. S., Herman, R. L., Troy, R. F.,  
416 Rosenlof, K., Thompson, T. L., Fridlind, A. M., Hudson, P. K., Cziczo, D. J., Heymsfield, A. J., Schmitt, C.  
417 and Wilson, J. C.: Ice Supersaturations Exceeding 100% at the Cold Tropical Tropopause: Implications for  
418 Cirrus Formation and Dehydration, *Atmos. Chem. Phys.*, *5*, 851-62, 2005.

419 Jost, H. J., et al.: In-situ observations of mid-latitude forest fire plumes deep in the stratosphere, *Geophys. Res. Lett.*,  
420 *31*, L11101, doi:10.1020/2003GL019253, 2004.

421 Kirk-Davidoff, D. B., Hints, E. J., Anderson, J. G., and Keith, D. W.: The effect of climate change on ozone  
422 depletion through changes in stratospheric water vapour, *Nature*, *402*, 399-401, doi:10.1038/46521, 1999.

423 Koshak, W. J., Cummins, K. L., Buechler, D. E., Vant-Hull B., Blakeslee, R. J., Williams, E. R., and H. S. Peterson:  
424 Variability of CONUS Lightning in 2003-12 and Associated Impacts, *J. Appl. Meteor. Climat.*, *54*, 15-  
425 41, doi:10.1175/JAMC-D-14-0072.1, 2015.

426 Livesey, N. J., Read, W. G., Wagner, P. A., Froidevaux, L., Lambert, A., Manney, G. L., Millan Valle, L. F.,  
427 Pumphrey, H. C., Santee, M. L., Schwartz, M. J., Wang, S., Fuller, R. A., Jarnot, R. F., Knosp, B. W., and  
428 Martinez, E.: Earth Observing System (EOS) Aura Microwave Limb Sounder (MLS) Version 4.2x Level 2  
429 data quality and description document, Tech. Rep. JPL D-33509 Rev. B, Version 4.2x-2.0, Jet Propulsion  
430 Laboratory, California Institute of Technology, Pasadena, CA, available online at:  
431 <http://mls.jpl.nasa.gov/data/datadocs.php> (last access: May 9, 2016), 2016.

432 Liu, C., Zipser, E. J., Cecil, D. J., Nesbitt, S. W., Sherwood, S.: *J. Appl. Meteorol. Climatol.* *47*, 2712: 2008.

433 Liu, N., and Liu, C.: Global distribution of deep convection reaching tropopause in 1 year GPM observations, *J.*  
434 *Geophys. Res. Atmos.*, *121*, doi:10.1002/2015JD024430, 2016.

435 May, R. D.: Open-path, near-infrared tunable diode laser spectrometer for atmospheric measurements of H<sub>2</sub>O, *J.*  
436 *Geophys. Res.*, *103*(D15), 19161-19172, doi:10.1029/98jd01678, 1998.

437 Moyer, E., Irion, F., Yung, Y., and Gunson, M.: ATMOS stratospheric deuterated water and implications for  
438 troposphere-stratosphere transport, *Geophys. Res. Lett.*, *23*(17), 2385-88, 1996.

439 Mullendore, G. L., Durran, D. R., and Holton, J. R.: Cross-tropopause tracer transport in midlatitude convection, *J.*  
440 *Geophys. Res.*, *110*, D06113, doi:10.1029/2004JD005059, 2005.

441 Mullendore, G. L., Homann, A. J., Bevers, K., and Schumacher, C.: Radar reflectivity as a proxy for convective  
442 mass transport, *J. Geophys. Res.*, *114*, D16103, doi:10.1029/2008JD011431, 2009.

443 Randel, W. J., K. Zhang, and R. Fu: What controls stratospheric water vapor in the NH summer monsoon regions?,  
444 *J. Geophys. Res.*, *120*, 7988–8001, doi:10.1002/2015JD023622, 2015.

445 Ravishankara, A. R.: Water Vapor in the Lower Stratosphere, *Science*, *337*, 809–810, doi: 10.1126/science.1227004,  
446 2012.

447 Ray, E. A., Rosenlof, K. H., Richard, E. C., Hudson, P. K., Cziczo, D. J., Loewenstein, M., Jost, H.-J., Lopez, J.,  
448 Ridley, B., Weinheimer, A., Montzka, D., Knapp, D., Wofsy, S. C., Daube, B. C., Gerbig, C., Xueref, I., and  
449 Herman, R. L.: Evidence of the effect of summertime midlatitude convection on the subtropical lower  
450 stratosphere from CRYSTAL-FACE tracer measurements, *J. Geophys. Res.*, *109*(D18), D18304, doi:  
451 10.1029/2004JD004655, 2004.

452 Read, W. G., et al.: Aura Microwave Limb Sounder upper tropospheric and lower stratospheric H<sub>2</sub>O and relative  
453 humidity with respect to ice validation, *J. Geophys. Res. Atmospheres*, *112*(D24), D24S35,  
454 doi:10.1029/2007jd008752, 2007.

455 Roach, W. T.: On the nature of the summit areas of severe storms in Oklahoma, *Q. J. R. Meteorol. Soc.*, *93*, 318–  
456 336, 1967.

457 Rodgers, C. D.: Inverse Methods for Atmospheric Sounding: Theory and Practice, World Science, London, 2000.

458 Rodgers, C. D., and Connor, B. J.: Intercomparison of Remote Sounding Instruments, *J. Geophys. Res.*, *108*, 4116,  
459 doi: 10.1029/2002JD002299, 2003.

460 Saha, S. et al.: The NCEP Climate Forecast System Version 2, *J. Climate*, *27*, 2185–2208, doi:10.1175/JCLI-D-12-  
461 00823.1, 2014.

462 Sargent, M. R., Smith, J. B., Sayres, D. S., and Anderson, J. G.: The roles of deep convection and extratropical  
463 mixing in the Tropical Tropopause Layer: An in situ measurement perspective, *J. Geophys. Res.*, *119*(21),  
464 12355-71, DOI:10.1002/2014JD022157, 2014.

465 Sayres, D. S., Pfister, L., Hanisco, T. F., Moyer, E. J., Smith, J. B., St. Clair, J. M., O'Brien, A. S., Witinski, M. F.,  
466 Legg, M., and Anderson, J. G.: Influence of convection on the water isotopic composition of the tropical  
467 tropopause layer and tropical stratosphere, *J. Geophys. Res.*, *115*, D00J20, doi:10.1029/2009JD013100, 2010.

468 Schwartz, M. J., Read, W. G., Santee, M. L., Livesey, N. J., Froidevaux, L., Lambert, A., and Manney, G. L.:  
469 Convectively injected water vapor in the North American summer lowermost stratosphere, *Geophys. Res.*  
470 *Lett.*, *40*, 2316-2321, doi:10.1002/grl.50421, 2013.

471 Scott, S. G., Bui, T. P., Chan, K. R., and Bowen, S. W.: The meteorological measurement system on the NASA ER-  
472 2 aircraft, *J. Atmos. Ocean. Tech.*, *7*, 525-40, 1990.

473 Shindell, D. T.: Climate and ozone response to increased stratospheric water vapor, *Geophys. Res. Lett.*, *28*, 1551-4,  
474 2001.

475 Smith, J. B., Sargent, M., Wilmoth, D. and Anderson, J. G.: Quantifying the Direct Convective Transport of  
476 Tropospheric Air to the Overworld Stratosphere, Abstract A51O-0288, presented at 2015, Fall Meeting, AGU,  
477 San Francisco, CA, 14-18 December, 2015.

478 Solomon, D. L., Bowman, K. P., and Homeyer, C. R.: Tropopause-Penetrating Convection from Three-Dimensional  
479 Gridded NEXRAD Data, *J. Appl. Met. Climat.*, 55, 465-78, DOI:10.1175/JAMC-D-15-0190.1, 2016.

480 Solomon, S., Rosenlof, K. H., Portmann, R. W., Daniel, J. S., Davis, S. M., Sanford, T. J., and Plattner, G.-K.:  
481 Contributions of Stratospheric Water Vapor to Decadal Changes in the Rate of Global Warming, *Science*,  
482 327(5970), 1219-1223, doi:10.1126/science.1182488, 2010.

483 Stohl, A., C. Forster, A. Frank, P. Seibert, and G. Wotawa: Technical note: The Lagrangian particle dispersion  
484 model FLEXPART version 6.2, *Atmos. Chem. Phys.*, 5, 2461-2474, doi: 10.5194/acp-5-2461-2005-  
485 supplement, 2005.

486 Toon, O. B., H. Maring, J. Dibb, R. Ferrare, D. J. Jacob, E. J. Jensen, Z. J. Luo, G. G. Mace, L. L. Pan, L. Pfister, K.  
487 H. Rosenlof, J. Redemann, J. S. Reid, H. B. Singh, A. M. Thompson, R. Yokelson, P. Minnis, G. Chen, K. W.  
488 Jucks, and A. Pszenny: Planning, implementation and scientific goals of the Studies of Emissions and  
489 Atmospheric Composition, Clouds and Climate Coupling by Regional Surveys (SEAC<sup>4</sup>RS) field mission, *J.*  
490 *Geophys. Res.*, 121, 4967-5009, doi:10.1002/2015JD024297, 2016.

491 Voemel, H., et al.: Balloon-borne observations of water vapor and ozone in the tropical upper troposphere and lower  
492 stratosphere, *J. Geophys. Res.*, 107(D14), pages ACL 8-1-ACL 8-16, DOI:10.1029/2001JD000707, 2002.  
493 Available online at <http://onlinelibrary.wiley.com/doi/10.1029/2001JD000707/full#jgrd8979-fig-0017>, 2002.

494 Wang, P. K., Moisture plumes above thunderstorm anvils and their contributions to cross-tropopause transport of  
495 water vapor in midlatitudes, *J. Geophys. Res.*, 108(D6), 4194, doi:10.1029/2002JD002581, 2003.

496 Webster, C. R., and Heymsfield, A. J.: Water Isotope Ratios D/H, <sup>18</sup>O/<sup>16</sup>O, <sup>17</sup>O/<sup>16</sup>O in and out of Clouds Map  
497 Dehydration Pathways, *Science*, 302, 1742, DOI: 10.1126/science.1089496, 2003.

498 **TABLES**

499

500 **Table 1** Summary of enhanced water vapor measurements in the overworld stratosphere during SEAC<sup>4</sup>RS\*. Dates  
 501 are NASA ER-2 aircraft flight dates in day-month-year format, and JLH Mark2 maximum water vapor mixing ratios  
 502 (ppmv) are shown for potential temperatures greater than 400 K (left) and in the range 380-400 K (right).

Date	max. water (ppmv)	Pot. Temp. (K)	Altitude (km)	max. water (ppmv)	Pot. Temp. (K)	Altitude (km)
	above 400 K	above 400 K	above 400 K	380-400K	380-400K	380-400K
8-Aug-2013	10.1	401.2	17.29	11.2	385.7	17.10
12-Aug-2013	8.0	400.1	17.08	13.2	388.1	16.86
14-Aug-2013	7.7	402.2	17.38	10.7	387.4	16.75
16-Aug-2013	7.0	400.2	17.14	12.2	387.3	16.82
27-Aug-2013	15.3	402.8	17.32	17.7	380.8	16.12
30-Aug-2013	9.2	400.2	17.27	12.0	390.0	16.81
2-Sep-2013	8.0	400.3	17.07	13.0	380.3	16.28
4-Sep-2013	6.3	405.0	17.57	10.8	380.2	16.32
6-Sep-2013	6.8	400.1	17.12	15.6	381.0	16.32
11-Sep-2013	7.7	400.2	17.13	10.2	381.0	16.22
13-Sep-2013	6.9	401.8	17.55	9.2	382.4	16.41

503 \* SEAC<sup>4</sup>RS = Studies of Emissions and Atmospheric Composition, Clouds and Climate Coupling by Regional  
 504 Surveys

505

506 **FIGURE CAPTIONS**

507

508 **Figure 1.** JLH Mark2 stratospheric water vapor profiles from 23 aircraft flights during SEAC<sup>4</sup>RS. This altitude  
 509 range includes the overworld stratosphere (potential temperature greater than 380 K) and lowermost stratosphere  
 510 (tropopause to 380 K). The majority of observations have mixing ratios less than 10 ppmv in the lowermost  
 511 stratosphere and less than 6 ppmv in the overworld stratosphere. Enhanced water measurements are the extreme  
 512 outliers with high water mixing ratios, with a threshold value of mean plus two standard deviations.  
 513

514

515 **Figure 2.** Distribution of JLH Mark2 water vapor at potential temperatures 380 K to 400 K in the overworld  
 516 stratosphere for all flights in the SEAC<sup>4</sup>RS mission (summer 2013). These potential temperatures correspond to  
 517 approximately 16.8 to 17.4 km altitude (99 to 90 hPa).  
 518

519

519 **Figure 3.** Distribution of JLH Mark2 water vapor at potential temperatures 400 K to 420 K in the overworld  
 520 stratosphere for all flights in the SEAC<sup>4</sup>RS mission (summer 2013). These potential temperatures correspond to  
 521 approximately 17.4 to 18.0 km altitude (90 to 80 hPa).  
 522

523

523 **Figure 4.** Distribution of Aura MLS v4.2 100-hPa H<sub>2</sub>O over CONUS (blue shaded box in insert), corresponding to  
 524 approximately 17 km altitude. The two histograms for July-August 2013 (blue asterisks and trace) and the previous  
 525 nine-summer MLS record, July-August 2004 through 2012 (red circles and trace) indicates that 2013 was drier than  
 526 average. The threshold for MLS-detected ‘enhanced water vapor’ (thick black vertical line) is set at 8 ppmv, same as  
 527 Schwartz et al. (2013), to exclude the larger population of measurements at 6 to 8 ppmv water vapor that may have

528 other sources.

529

530 **Figure 5.** Two-month mean map of Aura MLS v4.2 100-hPa H<sub>2</sub>O (color scale), corresponding to approximately 17  
531 km altitude, with superimposed MERRA horizontal winds (arrows) for July-August 2013 during the SEAC<sup>4</sup>RS time  
532 period. MLS observations of 100-hPa H<sub>2</sub>O greater than 8 ppmv in this two-month period are shown by the white  
533 circles.

534

535 **Figure 6.** Map and profiles of aircraft and satellite water vapor on 8 August 2013 over California (number 1 shown  
536 in dark blue) and Texas (number 2 shown in green). (a) Map of ER-2 aircraft flight track (solid colored trace) and  
537 nearly coincident Aura MLS geolocations (asterisks and lines). (b) ER-2 aircraft altitude profiles (solid colored  
538 trace) color-coded by dives and MLS times (horizontal lines). (c) Vertical profiles of *in situ* water vapor  
539 measurements from JLH Mark2 (dots) and MLS retrievals of water vapor (circles and lines). Some measurements  
540 exceed the threshold for enhanced water vapor of 8 ppmv for Aura MLS (after Schwartz et al., 2013), and the  
541 campaign-wide mean plus 2 st. dev. for JLH Mark 2, 9.7 ppmv at 380-400 K and 6.6 ppmv at 400-420 K.

542

543 **Figure 7.** Analysis of the 8 August 2013 NASA ER-2 aircraft flight. (a) Vertical profiles of JLH Mark2 *in situ* H<sub>2</sub>O.  
544 Back trajectories were initialized from all aircraft water measurements at 16 to 17.5 km altitude. (b) Example back  
545 trajectories (thin blue traces) and coincident overshooting convection (red). Along the NASA ER-2 flight track  
546 (orange line), enhanced water vapor was measured (thick blue lines). This figure identifies where trajectories and  
547 OT are coincident (red squares) within tolerances prescribed in Section 3.2. The green markers are overshooting  
548 convective tops within +/-3 hours of the red squares to indicate the main regions of convective overshooting during  
549 the seven days prior to the ER-2 flight and which of those regions appeared to contribute most to the water vapor  
550 enhancement measured on the flight. (c) Altitude plot of example back trajectories showing coincident overshooting  
551 (red squares). The green markers are overshooting convective tops within +/-3 hours of the red squares. The high  
552 resolution of the convective overshooting data meant that there could be multiple coincident convective  
553 overshooting cells for a single location on a back trajectory, (d) Days between OT and intercept by aircraft on 8  
554 August 2013.

555

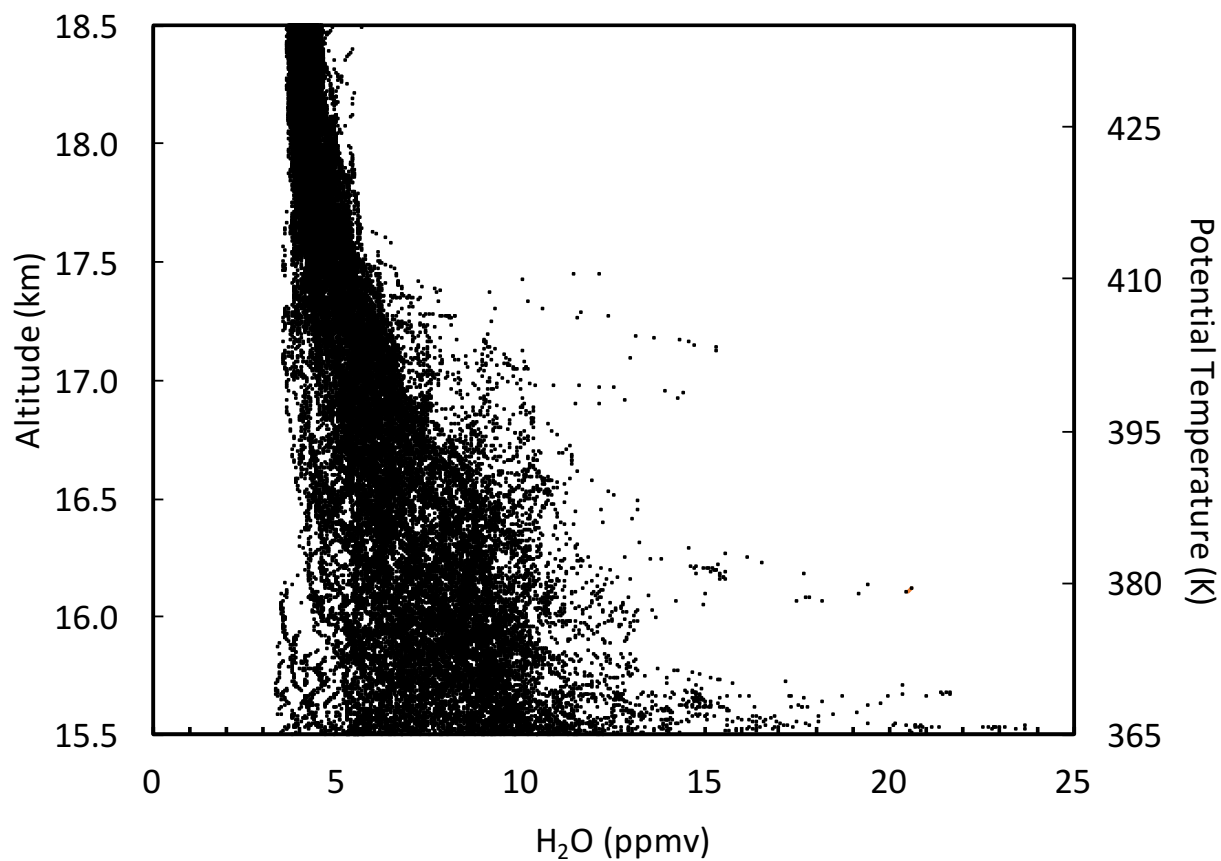
556 **Figure 8.** Analysis of the 16 August 2013 NASA ER-2 flight. (a) Vertical profiles of JLH Mark2 *in situ* H<sub>2</sub>O similar  
557 to Figure 7a, (b) Back trajectories from the aircraft path similar to Figure 7b, (c) Altitude plot of back trajectories  
558 showing coincident overshooting (red) and all overshooting within +/- 3 hours (green) similar to Figure 7c, (d) Days  
559 between OT and intercept by aircraft similar to Figure 7d.

560

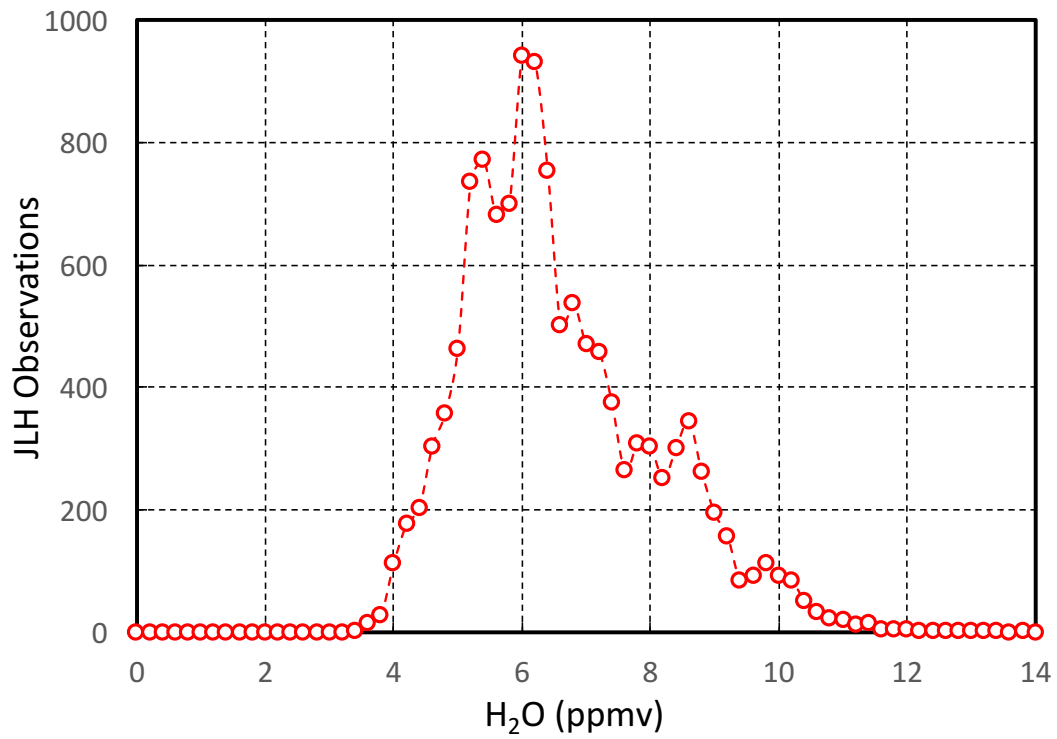
561 **Figure 9.** Analysis of the 27 August 2013 NASA ER-2 flight. (a) Vertical profiles of JLH Mark2 *in situ* H<sub>2</sub>O similar  
562 to Figure 7a, (b) Back trajectories from the aircraft path similar to Figure 7b, (c) Altitude plot of back trajectories  
563 showing coincident overshooting (red) and all overshooting within +/- 3 hours (green) similar to Figure 7c, (d) Days  
564 between OT and intercept by aircraft similar to Figure 7d.

565

566 **Figure 10.** Fraction of back trajectories that intersected OTs during the 7 previous days for the three SEAC<sup>4</sup>RS  
567 flights of 8 August (blue), 16 August (green) and 27 August 2013 (red) shown in Figures 7, 8 and 9, respectively.



568  
 569 **Figure 1.** JLH Mark2 stratospheric water vapor profiles from 23 aircraft flights during SEAC<sup>4</sup>RS. This altitude  
 570 range includes the overworld stratosphere (potential temperature greater than 380 K) and lowermost stratosphere  
 571 (tropopause to 380 K). The majority of observations have mixing ratios less than 10 ppmv in the lowermost  
 572 stratosphere and less than 6 ppmv in the overworld stratosphere. Enhanced water measurements are the extreme  
 573 outliers with high water mixing ratios, with a threshold value of mean plus two standard deviations.



574

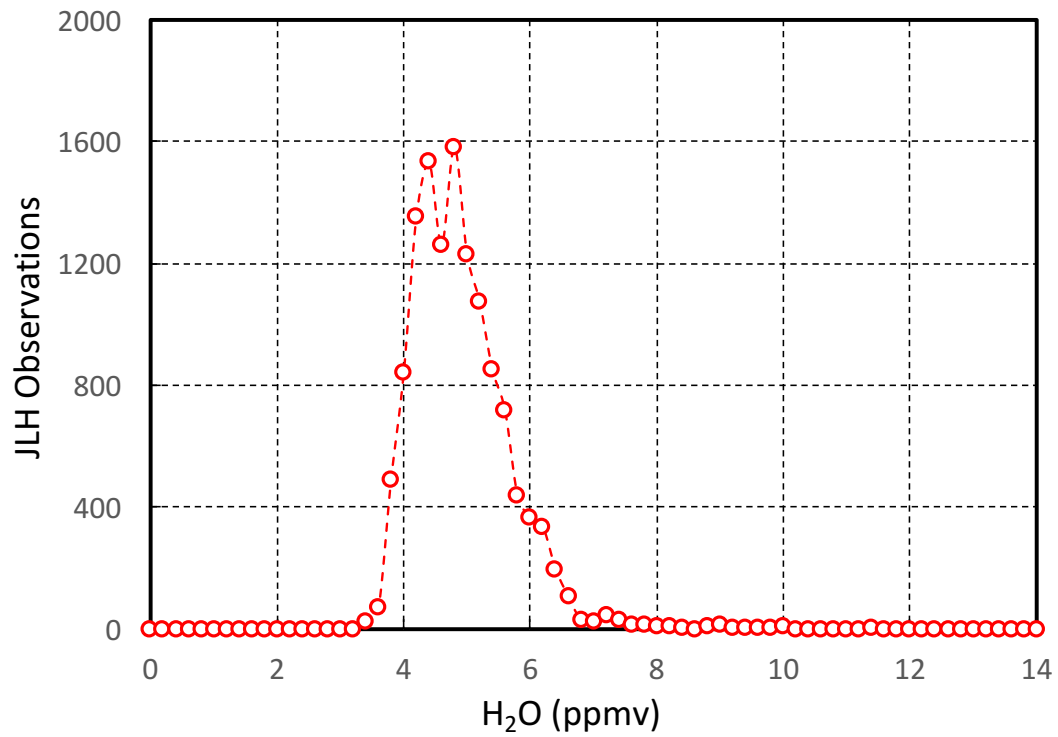
575

**Figure 2.** Distribution of JLH Mark2 water vapor at potential temperatures 380 K to 400 K in the overworld stratosphere for all flights in the SEAC<sup>4</sup>RS mission (summer 2013). These potential temperatures correspond to approximately 16.8 to 17.4 km altitude (99 to 90 hPa).

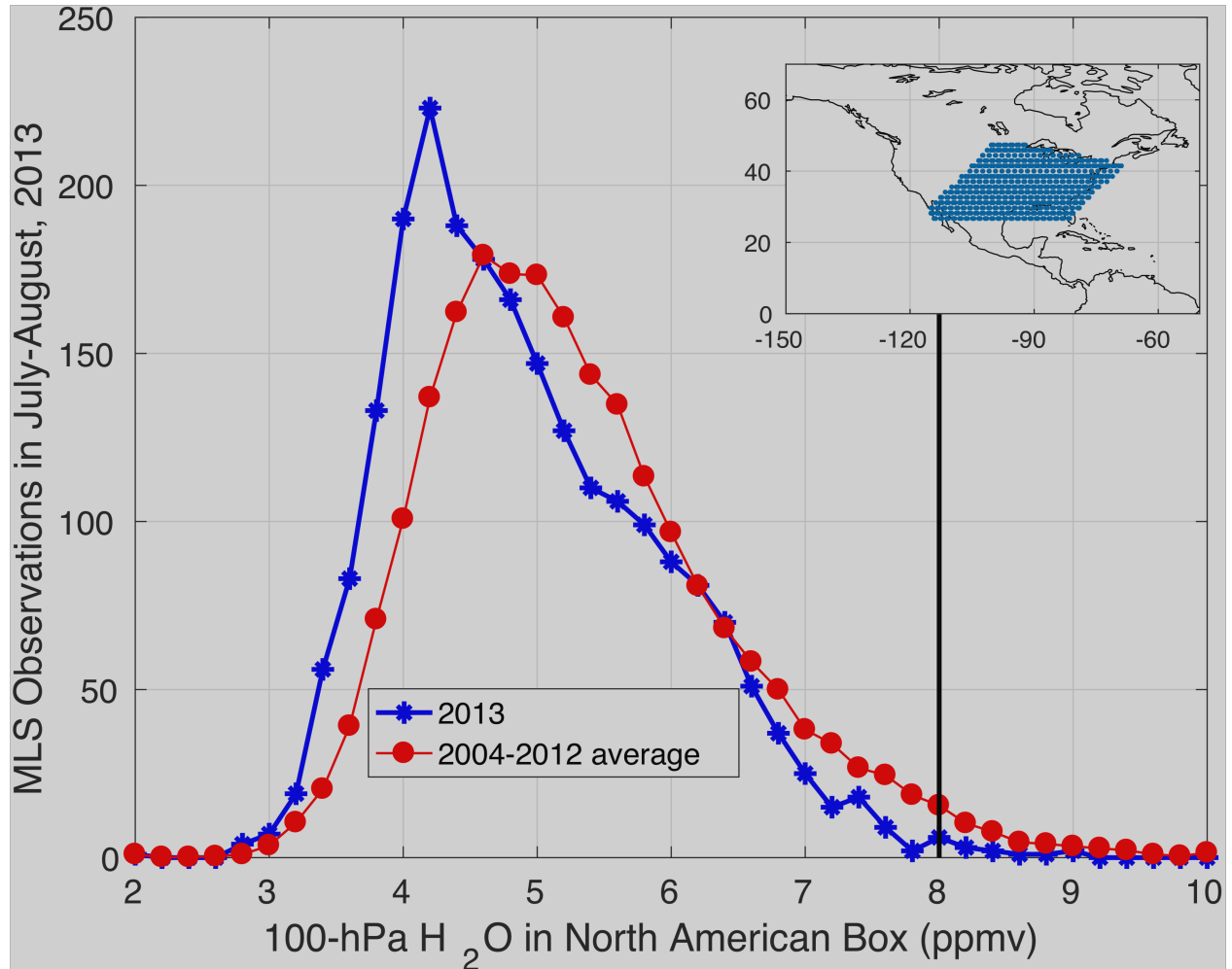
576

577

578



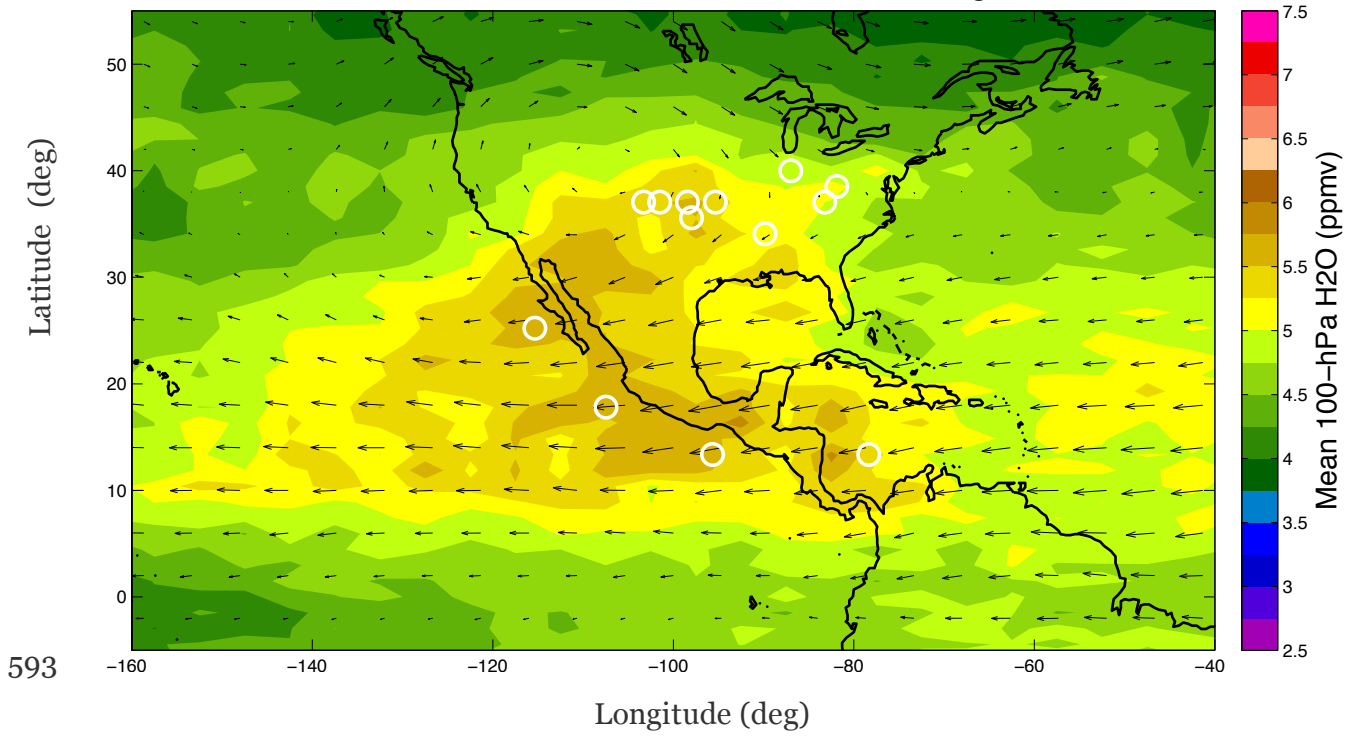
579  
 580 **Figure 3.** Distribution of JLH Mark2 water vapor at potential temperatures 400 K to 420 K in the overworld  
 581 stratosphere for all flights in the SEAC<sup>4</sup>RS mission (summer 2013). These potential temperatures correspond to  
 582 approximately 17.4 to 18.0 km altitude (90 to 80 hPa).  
 583



584  
585  
586  
587  
588  
589  
590  
591  
592

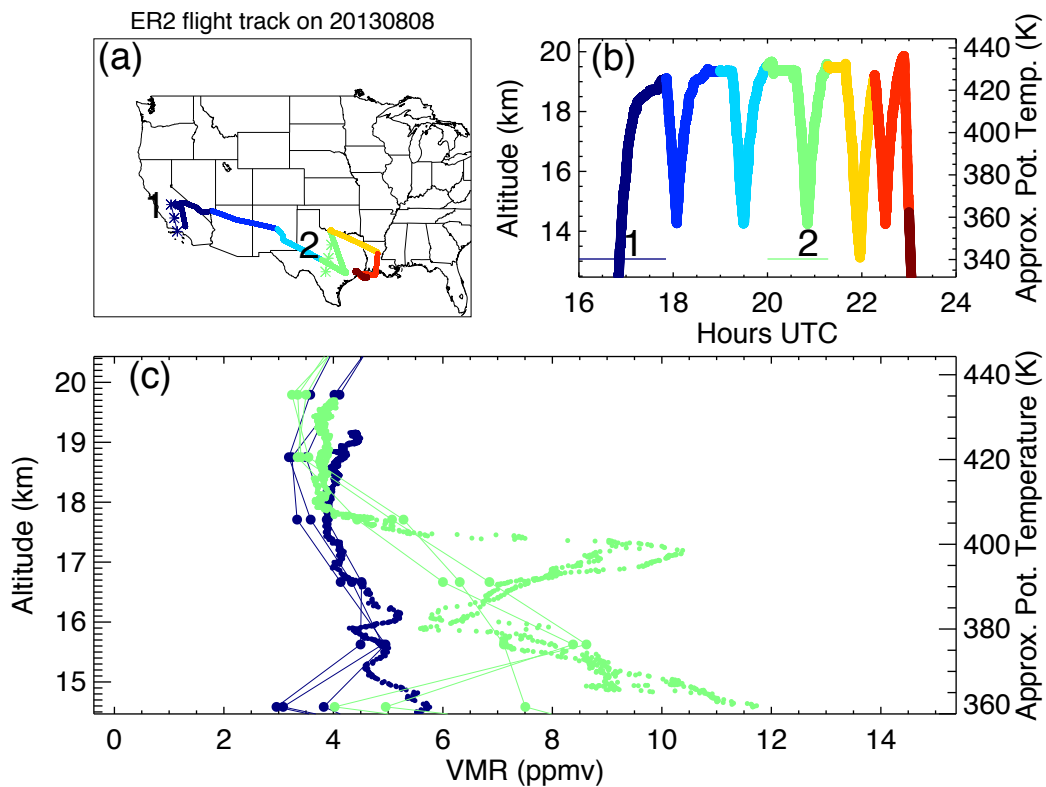
**Figure 4.** Distribution of Aura MLS v4.2 100-hPa H<sub>2</sub>O over CONUS (blue shaded box in insert), corresponding to approximately 17 km altitude. The two histograms for July-August 2013 (blue asterisks and trace) and the previous nine-summer MLS record, July-August 2004 through 2012 (red circles and trace) indicates that 2013 was drier than average. The threshold for MLS-detected ‘enhanced water vapor’ (thick black vertical line) is set at 8 ppmv, same as Schwartz et al. (2013), to exclude the larger population of measurements at 6 to 8 ppmv water vapor that may have other sources.

Mean 100-hPa H<sub>2</sub>O 01-Jul-2013 -- 31-Aug-2013

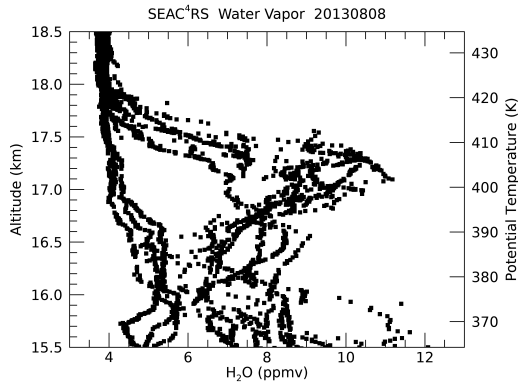


593

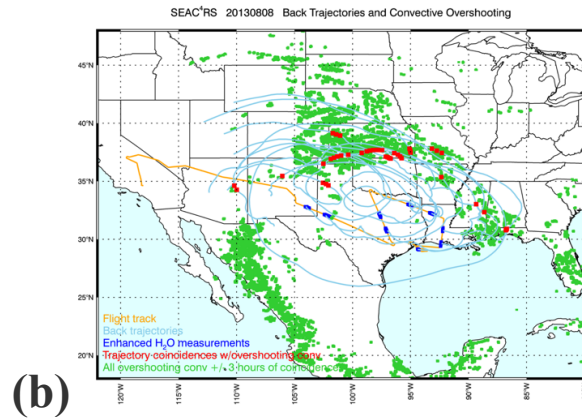
594 **Figure 5.** Two-month mean map of Aura MLS v4.2 100-hPa H<sub>2</sub>O (color scale), corresponding to approximately 17  
595 km altitude, with superimposed MERRA horizontal winds (arrows) for July-August 2013 during the SEAC<sup>4</sup>RS time  
596 period. MLS observations of 100-hPa H<sub>2</sub>O greater than 8 ppmv in this two-month period are shown by the white  
597 circles.



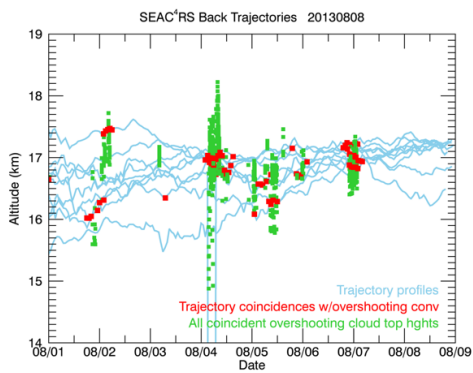
598  
 599 **Figure 6.** Map and profiles of aircraft and satellite water vapor on 8 August 2013 over California (number 1 shown  
 600 in dark blue) and Texas (number 2 shown in green). (a) Map of ER-2 aircraft flight track (solid colored trace) and  
 601 nearly coincident Aura MLS geolocations (asterisks and lines). (b) ER-2 aircraft altitude profiles (solid colored  
 602 trace) color-coded by dives and MLS times (horizontal lines). (c) Vertical profiles of *in situ* water vapor  
 603 measurements from JLH Mark2 (dots) and MLS retrievals of water vapor (circles and lines). Some measurements  
 604 exceed the threshold for enhanced water vapor of 8 ppmv for Aura MLS (after Schwartz et al., 2013), and the  
 605 campaign-wide mean plus 2 st. dev. for JLH Mark 2, 9.7 ppmv at 380-400 K and 6.6 ppmv at 400-420 K.  
 606



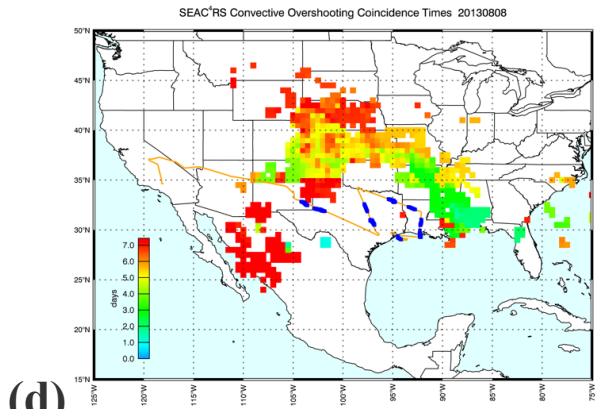
607 (a)



(b)



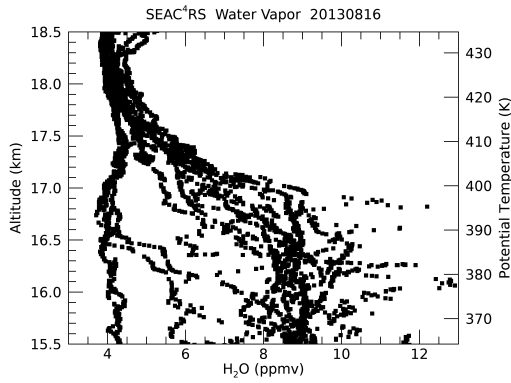
608 (c)



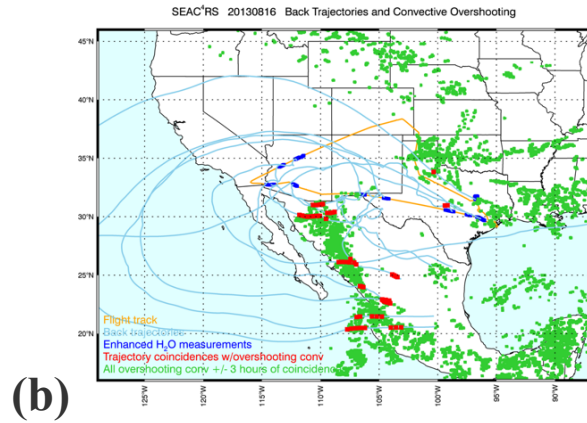
(d)

609 **Figure 7.** Analysis of the 8 August 2013 NASA ER-2 aircraft flight. (a) Vertical profiles of JLH Mark2 *in situ* H<sub>2</sub>O.  
 610 Back trajectories were initialized from all aircraft water measurements at 16 to 17.5 km altitude. (b) Example back  
 611 trajectories (thin blue traces) and coincident overshooting convection (red). Along the NASA ER-2 flight track  
 612 (orange line), enhanced water vapor was measured (thick blue lines). This figure identifies where trajectories and  
 613 OT are coincident (red squares) within tolerances prescribed in Section 3.2. The green markers are overshooting  
 614 convective tops within +/-3 hours of the red squares to indicate the main regions of convective overshooting during  
 615 the seven days prior to the ER-2 flight and which of those regions appeared to contribute most to the water vapor  
 616 enhancement measured on the flight. (c) Altitude plot of example back trajectories showing coincident overshooting  
 617 (red squares). The green markers are overshooting convective tops within +/-3 hours of the red squares. The high  
 618 resolution of the convective overshooting data meant that there could be multiple coincident convective  
 619 overshooting cells for a single location on a back trajectory, (d) Days between OT and intercept by aircraft on 8  
 620 August 2013.

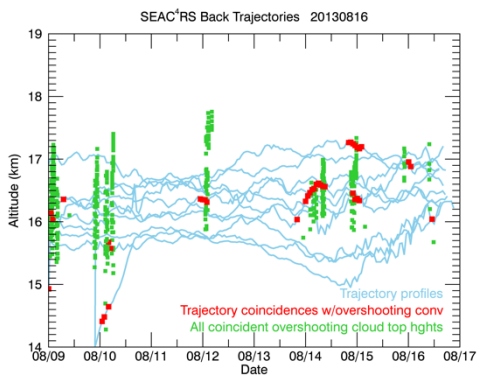
621



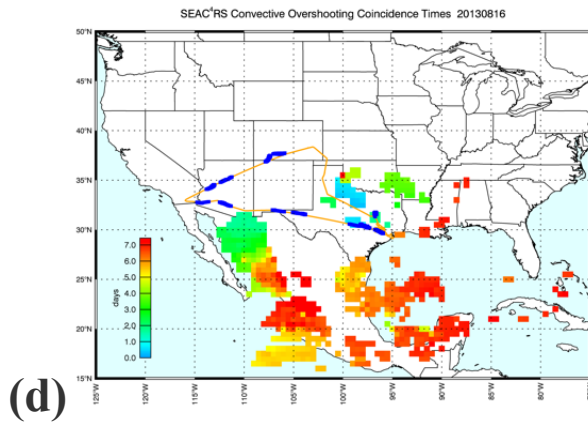
622 (a)



(b)

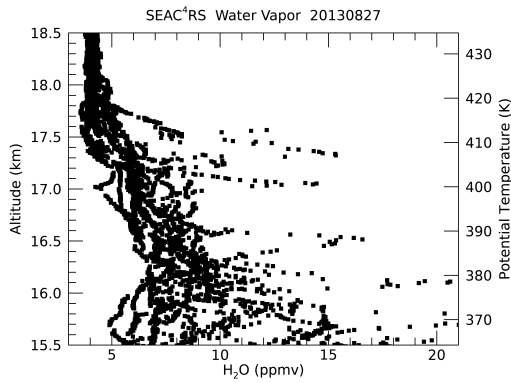


623 (c)

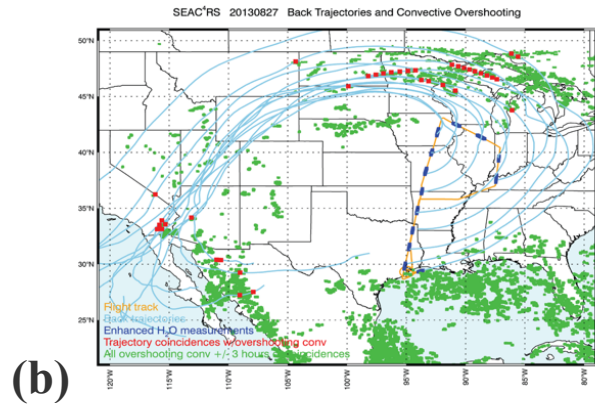


(d)

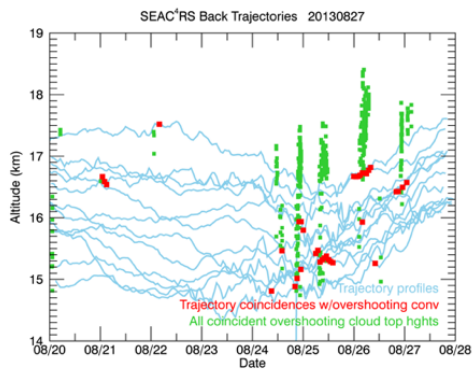
624 **Figure 8.** Analysis of the 16 August 2013 NASA ER-2 flight. (a) Vertical profiles of JLH Mark2 *in situ* H<sub>2</sub>O similar to Figure 7a, (b) Back trajectories from the aircraft path similar to Figure 7b, (c) Altitude plot of back trajectories  
625 showing coincident overshooting (red) and all overshooting within +/- 3 hours (green) similar to Figure 7c, (d) Days  
626 between OT and intercept by aircraft similar to Figure 7d.  
627  
628  
629



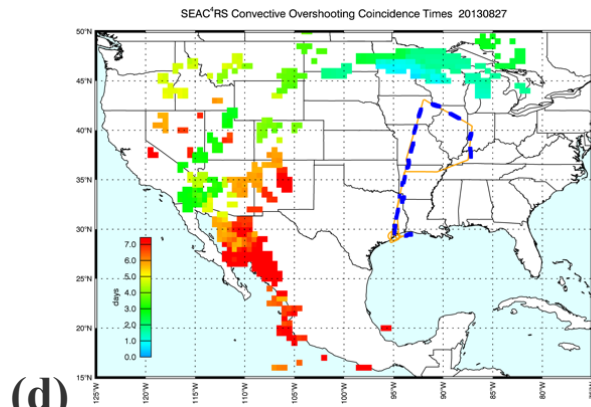
630 (a)



(b)

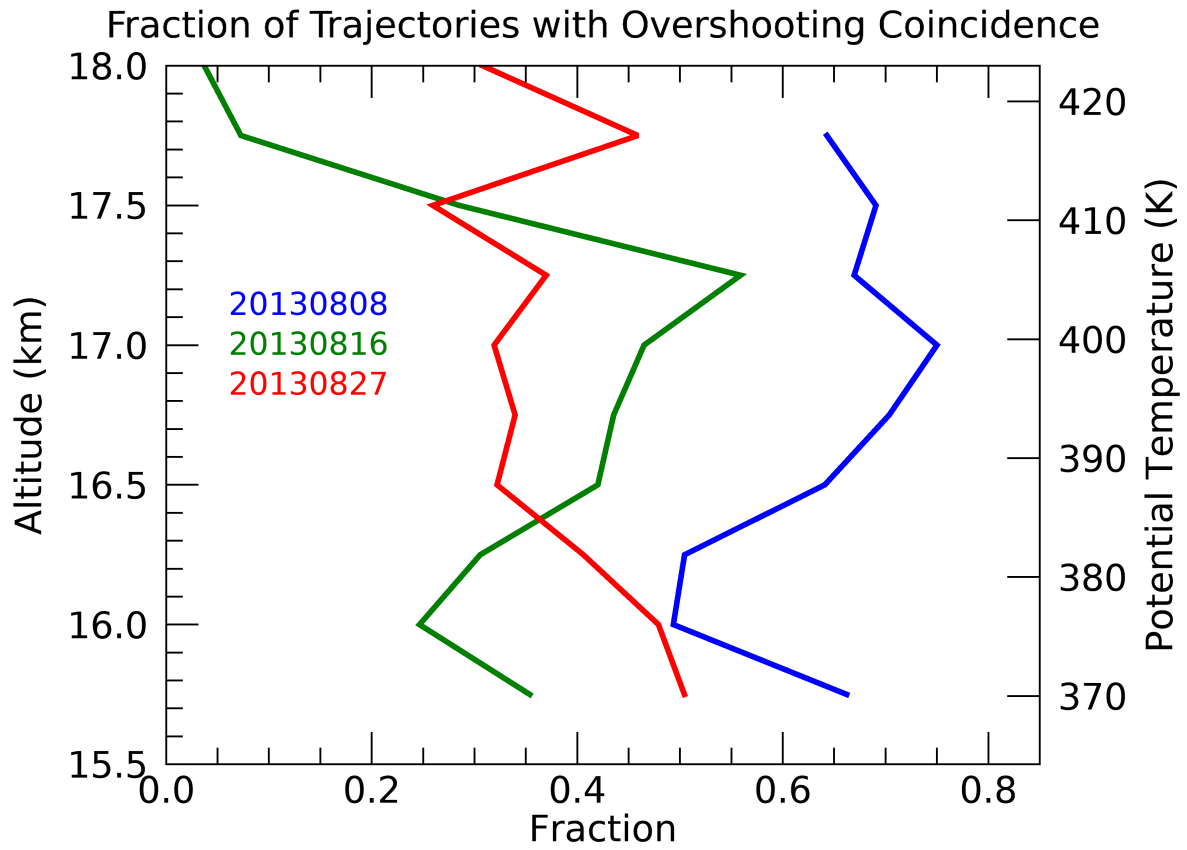


631 (c)



(d)

632 **Figure 9.** Analysis of the 27 August 2013 NASA ER-2 flight. (a) Vertical profiles of JLH Mark2 *in situ* H<sub>2</sub>O similar  
 633 to Figure 7a, (b) Back trajectories from the aircraft path similar to Figure 7b, (c) Altitude plot of back trajectories  
 634 showing coincident overshooting (red) and all overshooting within +/- 3 hours (green) similar to Figure 7c, (d)  
 635 Days between OT and intercept by aircraft similar to Figure 7d.  
 636



637

638

639

**Figure 10.** Fraction of back trajectories that intersected OTs during the 7 previous days for the three SEAC<sup>4</sup>RS flights of 8 August (blue), 16 August (green) and 27 August 2013 (red) shown in Figures 7, 8 and 9, respectively.